Research Square

Preprints are preliminary reports that have not undergone peer review.
They should not be considered conclusive, used to inform clinical practice,
or referenced by the media as validated information.

# A Co-Design Framework for UAV Logistics Infrastructure and Distributed UAV Swarm Scheduling

**Haoze Gu**
Harbin Institute of Technology
**Zhixin QI**
qizhx@hit.edu.cn

Harbin Institute of Technology
**Zejiao Dong**
Harbin Institute of Technology
**Abaho G. Gershome**
University of Rwanda

**Research Article**

**Keywords:** UAV logistics, Multi-Agent System, Distributed optimization, Alternating Direction Method of Multipliers, Spectral graph theory

**Posted Date:** April 30th, 2026

**DOI:** https://doi.org/10.21203/rs.3.rs-9532263/v1

**License:** This work is licensed under a Creative Commons Attribution 4.0 International License.
Read Full License

**Additional Declarations:** The authors declare no competing interests.

# A Co-Design Framework for UAV Logistics Infrastructure and Distributed UAV Swarm Scheduling

Haoze Gu[a], Zhixin Qi[a,*], Zejiao Dong[a], Abaho G. Gershome[b]

[a]*the Department of Transportation Science and Engineering, Harbin Institute of Technology, P.R. China*
[b]*the Department of Civil, Environmental and Geomatic Engineering, University of Rwanda, Republic of Rwanda.*

**Abstract**

In large-scale UAV logistics systems, distributed scheduling has emerged as a key approach to overcoming the scalability limitations of centralized architectures. However, existing studies primarily focus on improving optimization algorithms, while largely overlooking the fundamental constraints imposed by the underlying communication topology. In real urban environments, heterogeneous spatial distributions often lead to poorly connected networks, which in turn become a critical bottleneck limiting distributed coordination efficiency.This paper investigates how communication topology shapes distributed scheduling performance from the perspective of coupling transportation infrastructure and information interaction. Building upon algebraic graph theory and distributed optimization, we establish a quantitative relationship between network connectivity and the convergence rate of cooperative errors, and show that, under construction cost constraints, system performance is subject to an inherent structural upper bound. To address this limitation, we propose a topology optimization method that enhances connectivity under realistic spatial constraints, and further develop a topology-aware distributed scheduling framework that enables joint design of infrastructure and coordination mechanisms.Experiments based on real-world logistics networks demonstrate that modest topology enhancements can accelerate system convergence and reduce scheduling delays under high-load conditions. Ablation studies further confirm that network connectivity plays a key role in determining overall system performance.Overall, this work reveals the mechanism linking transportation infrastructure topology to distributed coordination efficiency, and provides a principled approach to upgrading infrastructure from passive physical assets to active computational topology resources, offering theoretical support for the integration of computing and networking in future intelligent transportation systems.

© 2026 Published by Elsevier Ltd.

*Keywords:* UAV logistics, Multi-Agent System, Distributed optimization, Alternating Direction Method of Multipliers, Spectral graph theory

## 1. Introduction

As the low-altitude economy and Urban Air Mobility (UAM) expand, scheduling large-scale UAV clusters in high-demand logistics scenarios has become a critical challenge in Intelligent Transportation Systems (ITS) [1, 2]. Faced with massive scheduling dimensions and highly dynamic demands, traditional centralized control architectures often encounter computational bottlenecks and communication delays. Consequently, upgrading logistics hubs into autonomous scheduling agents with local computing and communication capabilities is increasingly necessary. In this

*Corresponding author
*Email address:* qizhx@hit.edu.cn (Zhixin Qi)

context, Multi-Agent Systems (MAS) have been widely adopted for decentralized resource allocation, enhancing the scalability of large-scale UAV networks [3].

In multi-agent decentralized scheduling, hub nodes can only communicate locally through the underlying physical communication topology to gradually reach a global resource allocation consensus. However, control and network optimization theories indicate that the information diffusion efficiency and convergence rate of distributed algorithms are bounded by the algebraic connectivity (Fiedler value, $\lambda_2$) of the underlying communication graph Laplacian [4]. This implies that the physical topology of transportation infrastructure directly affects the congestion resilience and response speed of the upper-layer scheduling system.

UAV logistics networks have not yet been widely deployed, prompting a reconsideration of whether their design should follow the traditional location logic of ground transportation systems. Conventional logistics infrastructure is typically designed to adapt to geographical demand density and land-use constraints [5]. However, if UAV logistics hubs are viewed as agents with autonomous scheduling capabilities, the focus of location decisions shifts from purely geographic placement to interaction efficiency among agents. The traditional paradigm—emphasizing geographic location while neglecting computational topology—becomes insufficient. The requirements of these two transportation modes are inherently mismatched, making it unreasonable to directly apply existing ground logistics networks. Conversely, optimizing solely for agent interaction without considering spatial constraints is also impractical. From a theoretical perspective, Ramanujan graphs provide near-optimal spectral expansion under degree constraints, offering ideal topological conditions for agent interaction [6]. However, their purely algebraic construction does not align with real spatial constraints, preventing direct application in transportation systems.

Furthermore, in practical low-altitude logistics environments, multi-agent negotiation and consensus are not only constrained by geographical topology but also affected by communication delays and network limitations. As a result, distributed coordination processes may struggle to achieve perfect synchronization, and communication can be prematurely interrupted by physical clock constraints [7]. Under such imperfect infrastructure conditions, ensuring both efficiency and robustness of the multi-agent scheduling system remains a critical operations research challenge.

Motivated by these challenges, this paper proposes a Strategic-Operational Co-optimization Framework for UAV logistics hubs, as illustrated in Fig. 1. Unlike approaches that rely on existing geographical networks, this framework improves the algebraic connectivity of the communication topology under realistic spatial constraints. On this optimized physical foundation, an asynchronous decentralized scheduling mechanism is further developed to tolerate incomplete communication.

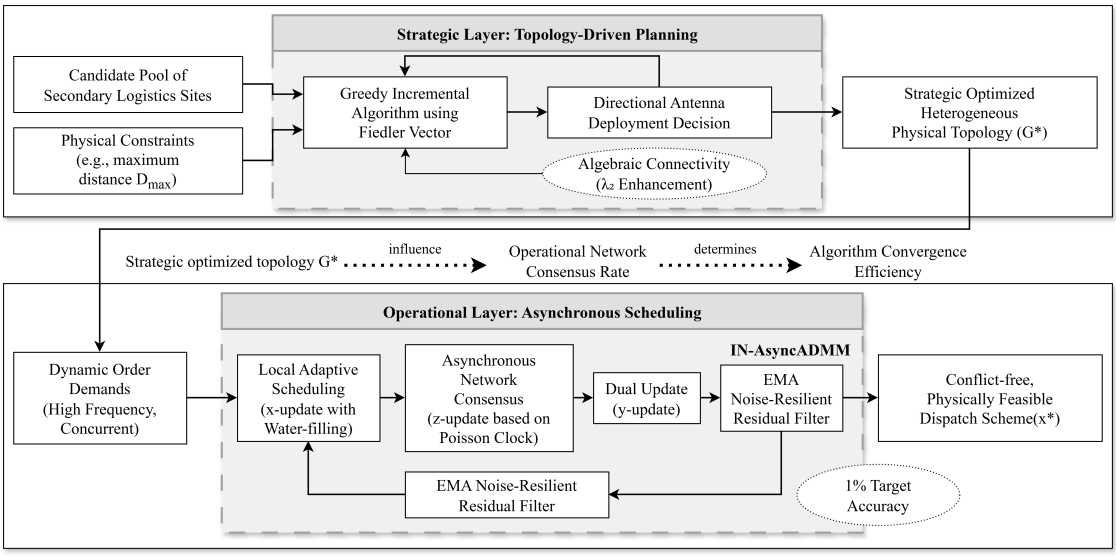



Figure 1: The Strategic-Operational Co-optimization Framework for UAV logistics hubs

The main contributions of this paper are summarized as follows:

1. **Reframing transportation infrastructure as a topology-driven computational system:** We move beyond

the conventional view of logistics infrastructure as purely physical assets by explicitly modeling it as a structural resource that governs information propagation and distributed coordination. This perspective reveals a previously overlooked coupling between infrastructure design and the efficiency of decentralized scheduling systems.

2. **Revealing topology as a fundamental bottleneck in real-world logistics networks:** Through a large-scale empirical analysis of over 3,000 delivery sites across 50 cities and 6 major logistics providers, we show that geographically-driven network structures exhibit a significant loss in algebraic connectivity (over 41% on average) relative to theoretical limits. This provides quantitative evidence that physical topology is a critical yet underexplored constraint on system-level coordination efficiency.
3. **A strategic-operational co-optimization framework for topology and distributed scheduling:** We propose an integrated framework that jointly optimizes physical topology and decentralized scheduling. At the strategic level, a spatially-constrained greedy edge-adding algorithm based on spectral perturbation theory enhances algebraic connectivity toward near-Ramanujan efficiency. At the operational level, a topology-aware asynchronous ADMM-based scheduling algorithm (IC-AsyncADMM) is developed to operate under incomplete communication, achieving near-centralized solution quality while reducing computational time under a 1% optimality gap.

The remainder of this paper is organized as follows. Section 2 reviews the related work. Section 3 formulates the multi-agent cooperative network design and resource allocation problem. Section 4 presents the Ramanujan-based theoretical analysis and the Fiedler-based topology optimization method under spatial constraints. Section 5 details the asynchronous distributed scheduling algorithm. Section 6 provides comprehensive experimental validation using real-world data. Finally, Section 7 concludes the paper.

## 2. Related Work

### *2.1. Intelligent Evolution of Urban Low-Altitude Logistics Infrastructure*

In early infrastructure planning frameworks, logistics hubs were conceptualized solely as passive geographic nodes for parcel collection and distribution. The rapid advancement of Urban Air Mobility (UAM for brief) has driven a fundamental shift in logistics networks, extending beyond ground-based operations to airspace integration, and evolving from standalone physical transport assets into highly complex Cyber-Physical Systems (CPS for brief) [8, 9]. For instance, Lu [10] identifies a clear shift in aviation hub research, from isolated single-site location selection to integrated complex network planning. Zhang [11] develops a two-layer hub location model subject to flight range and coverage constraints, while Ditta [12] constructs a 3D spatial network (3D-UAN for brief) that incorporates location-specific factors from a physical collision avoidance perspective.

While these emerging planning approaches have demonstrated promising performance in low-altitude traffic management, they remain largely rooted in the traditional facility location paradigm. Most model hubs as static geographic nodes, with rare consideration of their autonomous computing and scheduling capabilities through an agent-based lens. As a result, these frameworks fail to systematically account for the physical topology features required to support robust multi-agent collaboration during the location selection process.

When UAV hubs are modeled as agents with autonomous computing and decision-making capabilities, however, significant computational complexity challenges emerge under large-scale dynamic demand. This has driven the evolution of low-altitude traffic systems toward decentralized, autonomous scheduling architectures. In recent years, a growing body of work has begun to explore this paradigm shift. Onat [13], for example, proposes deploying vertiports as smart nodes to enable local capacity computation and resource allocation, while Kiran [14] leverages vehicle-mounted hubs to deliver grid computing support for 3D airspace operations.

With the proliferation of edge computing, distributed scheduling algorithms have been widely adopted for trajectory planning and task offloading workflows. Zhong [15] applies the Alternating Direction Method of Multipliers (ADMM for brief) algorithm to address the distributed consensus problem in multi-UAV role assignment, achieving significant reductions in system latency. Zheng [16] further develops a spatiotemporal trajectory optimization framework that integrates ADMM with differential dynamic programming. While distributed scheduling has emerged as the dominant design paradigm for these systems, recent work by Qiu et al. [17] highlights that multi-UAV collaboration efficiency is highly dependent on the underlying physical interaction topology. Despite this finding, mainstream

infrastructure planning frameworks still treat this underlying interaction topology as a fixed byproduct of physical location selection. This siloed design prioritizes spatial proximity while neglecting computational topology requirements, often resulting in complex distributed algorithms operating on suboptimal network structures in real-world deployment.

### 2.2. Topology Bottleneck and Algebraic Limits of Decentralized Scheduling

In multi-agent collaborative systems, the convergence rate of consensus-based decentralized algorithms (including ADMM) is subject to a fundamental theoretical upper bound. This bound is strictly constrained by the Laplacian spectrum of the underlying interaction graph, most notably the graph's algebraic connectivity (Fiedler value, $\lambda_2$) [18, 19].

To address this bottleneck, the majority of existing work focuses on optimizing the internal update rules of these algorithms. For example, Doostmohammadian [19] develops a Heavy-Ball Nonlinear Perturbation Gradient Tracking (HBNP-GT for brief) algorithm to mitigate the effects of network nonlinearities. Shrestha [20] introduces coarse quantization and error feedback mechanisms for asynchronous ADMM implementations to reduce communication overhead, and Doerks [21] leverages Graph Neural Networks (GNNs for brief) to adaptively learn optimal step sizes and interaction matrices. While these approaches have achieved notable performance improvements on suboptimal topologies, traffic infrastructure is subject to fixed location constraints and long network construction cycles. For such long-lived, capital-intensive infrastructure, directly enhancing the algebraic connectivity of the physical network via upfront infrastructure planning represents a far more fundamental solution.

In theoretical computer science and spectral graph theory, expander graphs—most notably Ramanujan graphs—have been proven to deliver near-optimal algebraic connectivity and minimal average path lengths under fixed node degree constraints [22]. Work by Li [23] further demonstrates that even approximate unbalanced expander graphs can guarantee robust connectivity in spatial distributed networks, while simultaneously delivering substantial reductions in overall communication energy costs. However, Ramanujan graphs constructed via purely algebraic methods (such as those based on algebraic group theory) frequently generate self-loops or multi-edges, and require physical links between nodes separated by extreme Euclidean distances [24]. For real-world traffic networks constrained by transmission power limits and line-of-sight requirements, such topologies are entirely infeasible.

In fact, maximizing algebraic connectivity under explicit 3D spatial constraints has been proven to be a canonical NP-hard problem [25]. Critically, algebraic connectivity is highly sensitive to physical spatial constraints, meaning system performance cannot rely solely on adaptive topology remediation during runtime [26]. Instead, hard spatial constraints and spectral performance requirements must be integrated into a unified planning framework during the initial hub deployment phase.

### 2.3. Joint Optimization Evolution of Physical Topology and Cooperative Algorithms

To resolve this disconnect between spatial constraints and algebraic performance limits, the network topology must be repositioned from a pre-defined static constant to a core decision variable in the planning process. Gross [27] was among the first to explicitly note that in large-scale discrete interconnected systems, the underlying topology must be co-optimized alongside distributed control laws. Subsequent work by Zhang [28] further confirms that even for optimal dual acceleration algorithms, sample complexity and convergence bounds cannot exceed the performance limits imposed by the network condition number $\kappa(L)$. To address this, Lu [29] develops an inverse construction method via Laplacian energy minimization, which provides a convex relaxation pathway for generating networks with high algebraic connectivity.

In recent years, the co-design of underlying interaction topologies and algorithm parameters has emerged as a key theoretical frontier [30]. In resource-constrained scenarios, formulating this problem as a Mixed-Integer Nonlinear Programming (MINLP for brief) model has proven to be an effective approach for enabling deep coupling between computing and network resources [31]. Furthermore, ADMM has evolved beyond its role as a core algorithm for distributed scheduling, and is now being innovatively applied to solve complex topology optimization problems. Recent work by Wang, Shen, and Hasanzadeh, for instance, formulates topology design as either a Mixed-Integer Semidefinite Programming (MISDP for brief) or Mixed-Integer Quadratic Programming (MIQP for brief) problem, and uses ADMM to relax and solve the discrete Boolean variables, maximizing consensus speed while reducing communication overhead [32, 33, 34].

However, these existing topology-algorithm co-design frameworks focus primarily on pure wireless communication networks or abstract learning spaces with high degrees of design freedom. They do not account for the strict real-world geographic distance constraints inherent to capital-intensive physical traffic infrastructure such as UAV logistics hubs. Specifically, there is a notable absence of work in the existing literature that integrates the physical constraints of 2D/3D geographic networks, the extreme spectral properties of Ramanujan graphs, and asynchronous scheduling algorithms robust to incomplete communication, to enable real-world implementation of topology-algorithm co-design for intelligent transportation infrastructure. This paper addresses this critical research gap by proposing a Strategic-Operational Co-optimization Framework as a practical, implementable solution.

## 3. Problem Description and Mathematical Modeling

### *3.1. Problem Description of Strategic-Operational Co-design*

Urban Air Mobility (UAM for brief) logistics is developing on a large scale. We can rely on existing ground delivery site networks and upgrade them. We can upgrade them into autonomous scheduling agents with distributed computing abilities. This can accurately respond to dynamic high-demand logistics needs. It can also effectively use existing traffic infrastructure resources and significantly reduce early deployment costs. However, traditional traffic facility planning is usually based only on geographical location and demand density. This separates the physical spatial location from the interaction topology of the upper-layer multi-agent cooperative architecture. In large-scale UAV cluster scheduling scenarios with high demand, the underlying traffic network topology may lack good algebraic connectivity. If so, it will not only cause a huge increase in the convergence delay of cooperative scheduling. It will also severely weaken the logistics network's anti-congestion and recovery abilities when facing sudden high demands.

To overcome the separation between physical infrastructure upgrades and information space, this paper formulates a two-stage framework. We formulate the construction and dynamic resource allocation of the UAV logistics hub network as a **Strategic-Operational Co-optimization Framework**:

- **Strategic Layer (Topology Design):** We select some nodes from existing delivery candidate sites. We upgrade them into UAV hub agents with autonomous scheduling abilities. Under given geographical location and construction cost constraints, we design the cooperative interaction topology among hubs. The core purpose is to build a network base with higher connectivity efficiency and stronger robustness. This serves the multi-agent decentralized scheduling at the physical level.
- **Operational Layer (High-Demand Order Scheduling):** Based on the physical interaction topology, we build a logistics resource allocation model. This model considers multi-hub capacity limits and global task demands. By decoupling global constraints, we transform traditional centralized allocation into decentralized cooperative scheduling based on local information interaction.

### *3.2. Strategic Layer: Cooperative Topology Modeling of UAV Logistics Hubs*

At the strategic layer, we first strictly define the urban low-altitude logistics network from the perspective of algebraic graph theory. Let the selected UAV hub network from the candidate pool be an undirected simple graph $\mathcal{G} = (\mathcal{V}, \mathcal{E})$. The vertex set $\mathcal{V} = \{\mathcal{V}_1, \mathcal{V}_2, \ldots, \mathcal{V}_N\}$ represents UAV hub agents with autonomous scheduling abilities. The edge set $\mathcal{E} \subseteq \mathcal{V} \times \mathcal{V}$ represents the effective cooperative interaction links built between hubs.

For graph $\mathcal{G}$, its adjacency matrix is defined as $A \in \mathbb{R}^{N\times N}$. If $(\mathcal{V}_i, \mathcal{V}_j) \in \mathcal{E}$, then $A_{ij} = 1$; otherwise, $A_{ij} = 0$. The degree matrix is defined as $D = \mathrm{diag}(d_1, d_2, \ldots, d_N)$. Here, $d_i = \sum_{j=1}^{N} A_{ij}$ is the degree of hub $\mathcal{V}_i$ in graph $\mathcal{G}$. We introduce the Graph Laplacian to describe the global cooperative flow efficiency of the traffic network:

$$L = D - A \tag{1}$$

Since $\mathcal{G}$ is an undirected connected graph, its Laplacian matrix $L$ is a real symmetric positive semi-definite matrix. Its eigenvalues $\lambda_i(L)$ satisfy the following order relation:

$$0 = \lambda_1(L) < \lambda_2(L) \leq \lambda_3(L) \leq \cdots \leq \lambda_N(L). \tag{2}$$

The second smallest eigenvalue $\lambda_2(L)$ is called Algebraic Connectivity. It can be strictly described by the Rayleigh quotient [35]:

$$\lambda_2(L_{\mathcal{G}}) = \min_{\mathbf{x}\perp\mathbf{1},\|\mathbf{x}\|_2=1} \mathbf{x}^\top L_{\mathcal{G}}\mathbf{x}. \tag{3}$$

Algebraic connectivity $\lambda_2(L)$ plays a core decisive role in UAV hub planning and distributed scheduling acceleration. Its strong coupling mechanism with the acceleration effect of subsequent scheduling algorithms will be strictly derived in Section 5. Based on this, we first introduce the following key topology optimization conclusion:

**Lemma 1** (Optimal Topology Condition)**.** *Given a UAV hub set $\mathcal{V} = \{\mathcal{V}_1, \mathcal{V}_2, \ldots, \mathcal{V}_N\}$, suppose any hub $\mathcal{V}_i \in \mathcal{V}$ satisfies the physical degree constraint $\deg(\mathcal{V}_i) \le d \in \mathbb{R}_+$. The optimal topology $\mathcal{G}^* = (\mathcal{V}^*, \mathcal{E}^*)$ must maximize its algebraic connectivity among all feasible topology structures:*

$$\lambda_2(L^*) = \sup\{\lambda_2(L) \mid \mathcal{G} = (\mathcal{V}, \mathcal{E}),\ \forall \mathcal{V}_i \in \mathcal{V}, \deg(\mathcal{V}_i) \le d\}. \tag{4}$$

Here, the constraint $\deg(\mathcal{V}_i) \le d$ directly maps the concurrent communication hardware limits of UAV hubs as edge computing nodes. A graph $\mathcal{G}$ satisfying this condition is called a $d$-bounded graph.

### *3.3. Operational Layer: Multi-Hub Cooperative Scheduling Modeling and Distributed Equivalent Reconstruction*

After establishing the cooperative topology $\mathcal{G}$ at the strategic layer, the operational layer needs to handle high-demand dynamic logistics needs on this physical base. Let $\mathcal{D} = \{1, 2, \ldots, M\}$ be the set of sudden delivery tasks randomly generated in urban space. We define a binary decision variable $x_{ij} \in \{0, 1\}$ to indicate whether hub $\mathcal{V}_i$ dispatches a UAV to task $j$. Let $\mathbf{x}_i = [x_{i1}, x_{i2}, \ldots, x_{iM}]^\top \in \mathbb{R}^M$ be the internal scheduling strategy vector of hub $\mathcal{V}_i$.

The system's physical feasibility in high-frequency logistics scenarios is dominated by two types of hard constraints. First, the number of landing pads and standby UAVs at each hub is limited by the local capacity $C_i > 0$. Second, each task $j \in \mathcal{D}$ needs exactly one UAV to complete the delivery. Let $\mathbf{c}_i \in \mathbb{R}^M_{++}$ be the comprehensive travel cost vector for hub $\mathcal{V}_i$ to execute tasks. The centralized optimal resource allocation problem is initially modeled as the following continuous Linear Programming (LP for brief):

$$\min_{\{\mathbf{x}_i\}_{i=1}^N} \quad \sum_{i=1}^N \mathbf{c}_i^\top \mathbf{x}_i \tag{5}$$

$$\text{s.t.} \quad \sum_{i=1}^N \mathbf{x}_i = \mathbf{1}, \quad \text{(Unique allocation for global tasks)} \tag{6}$$

$$\mathbf{1}^\top \mathbf{x}_i \le C_i, \quad \forall i \in \mathcal{V}, \quad \text{(Local hub capacity limits)} \tag{7}$$

$$\mathbf{x}_i \ge \mathbf{0}, \quad \forall i \in \mathcal{V}. \tag{8}$$

In the above model, we have relaxed the 0-1 integer constraint into a continuous non-negative constraint. Based on Total Unimodularity (TUM for brief) in traffic network flow theory, we present the following key lemma2:

**Lemma 2** (Integral Optimality of the Relaxed Assignment LP)**.** *Suppose the capacity parameter of each hub is $C_i \in \mathbb{Z}_{\ge 0}$. The constraint matrix of the model forms a bipartite graph incidence matrix and satisfies total unimodularity. Therefore, all extreme point solutions of the above continuous linear programming are naturally integer vectors. Thus, continuous relaxation does not change the optimal solution of the original integer programming problem. That is, $\mathbf{x}_i^* \in \{0, 1\}^M$ automatically holds.*

*(The detailed proof is in Appendix.)*

However, Equation (6) forms a global rigid constraint that strongly couples all nodes. To achieve true autonomous distributed scheduling on topology $\mathcal{G}$, we must decouple the constraints mathematically. To do this, we first encapsulate the local physical limits of each hub into an independent feasible set:

$$\tilde{\mathcal{X}}_i = \left\{\mathbf{x}_i \in \mathbb{R}^M \mid \mathbf{x}_i \ge \mathbf{0}, \mathbf{1}^\top \mathbf{x}_i \le C_i\right\}. \tag{9}$$

Furthermore, we aim to break the global variable coupling dilemma caused by $\sum_{i=1}^{N} \mathbf{x}_i = \mathbf{1}$ in mathematical calculation. We introduce an auxiliary consensus variable $\mathbf{z}_i \in \mathbb{R}^M$. This variable represents the cooperative decision state reached by hub $\mathcal{V}_i$ after local communication interaction with other agents. At this time, the original centralized programming is mathematically strictly equivalent to the following distributed form:

$$\min_{\{\mathbf{x}_i \in \tilde{\mathcal{X}}_i\}, \{\mathbf{z}_i\}} \quad \sum_{i=1}^{N} \mathbf{c}_i^\top \mathbf{x}_i \tag{10}$$

$$\text{s.t.} \quad \mathbf{x}_i = \mathbf{z}_i, \quad \forall i \in \mathcal{V}, \tag{11}$$

$$\sum_{i=1}^{N} \mathbf{z}_i = \mathbf{1}. \tag{12}$$

The reconstructed equivalent problem (10)-(12) establishes a standard mathematical framework for designing decentralized cooperative algorithms later. Under this framework, the efficiency of system scheduling will completely get rid of the dependence on an omniscient central processing unit. Instead, it will be achieved through local information interaction among multi-agents. The response efficiency and anti-congestion ability of this system-level cooperation will be deeply tied to the algebraic properties of the underlying physical topology $\mathcal{G}$.

## 4. Strategic Layer: Topology-Driven Logistics Infrastructure Planning

The two-layer model built in Section 3 shows a clear fact. Under high-demand orders, the decentralized cooperative efficiency of logistics networks is directly limited by the algebraic connectivity of the underlying physical topology $\mathcal{G}$. Traditional urban traffic infrastructure planning is mainly limited by geographical demand density and land resources. The network topology is often just a passive byproduct. However, in UAV logistics networks, the cooperative architecture between hubs is not just a set of physical links. It is a core decision variable that determines the performance of distributed scheduling algorithms.

Starting from spectral graph theory, this section first derives the theoretical upper bound of algebraic connectivity under physical degree limits. Then, we consider geographical distance constraints and the hardware cost of directional antennas in real urban traffic networks. We propose an incremental topology optimization algorithm based on spectral perturbation theory. This helps to build a highly connected infrastructure network.

### *4.1. Theoretical Benchmark of Algebraic Connectivity and Ramanujan Limit*

The information diffusion rate in distributed scheduling is strictly limited by the second smallest eigenvalue $\lambda_2(L)$ of the graph Laplacian matrix $L$. In theory, we can increase $\lambda_2(L)$ by adding communication links. But in real traffic engineering, UAV hubs have limits on antennas, processing power, and construction costs. We abstract these physical limits as a maximum node degree constraint $\deg(\mathcal{V}_i) \leq d$. This means the network topology must be a $d$-bounded graph. Under this condition, the algebraic connectivity has the following theoretical limit:

**Theorem 1** (Theoretical Upper Bound of Algebraic Connectivity for UAV Hubs)**.** *Given a physical construction constraint $d \geq 3$, suppose we have a connected $d$-bounded network topology $\mathcal{G}_N$ with $N$ UAV hubs. Its algebraic connectivity $\lambda_2(L)$ strictly meets the following bound:*

$$\lambda_2(L) \leq d - 2\sqrt{d-1} + O\left(\frac{1}{\log_{d-1} N}\right). \tag{13}$$

*Specifically, when the number of nodes $N \to \infty$ in the urban UAV logistics network, the system's algebraic connectivity has an asymptotic supremum (Alon-Boppana Bound):*

$$\limsup_{N\to\infty} \lambda_2(L) \leq d - 2\sqrt{d-1}. \tag{14}$$

*(The detailed proof of Theorem 1 is in Appendix. This proof is based on continuously adding links to the physical topology to approach a d-regular graph. It then uses the Nilli test vector to scale the spectral gap of the finite graph's adjacency matrix.)*

Theorem 1 defines the theoretical upper limit of the logistics network's cooperative efficiency under a given construction cost. In algebraic graph theory, a graph structure that can exactly reach this asymptotic limit is called a Ramanujan Graph:

**Theorem 2** (Optimal Infrastructure: Ramanujan Topology)**.** *Suppose all non-trivial adjacency eigenvalues of a d-regular traffic topology $\mathcal{G}$ satisfy $|\mu_i(A)| \leq 2\sqrt{d-1}$ $(i \geq 2)$. Then it is called a Ramanujan graph. Combined with the spectral mapping theorem, its algebraic connectivity exactly reaches the physical limit under the degree constraint: $\lambda_2(L) \geq d - 2\sqrt{d-1}$.*

To generate the theoretically optimal topology, we can use the Lubotzky-Phillips-Sarnak (LPS for brief) algebraic group construction method. This method finds the solution set of a specific Diophantine equation. It then maps it to the generators of a special linear group. This can deterministically construct a Ramanujan graph. *(The complete algebraic steps of using the LPS method to generate the isomorphic mapping of UAV hubs are in Appendix)*

### *4.2. Fiedler Greedy Incremental Planning Algorithm under Spatial Constraints*

The LPS method provides an asymptotic optimal theoretical benchmark. However, its generated graph structure is only an optimal solution at the abstract algebraic level. In such algebraic graphs, we often see topology structures that violate physical rules. These include super-long spatial edges, self-loops, and disconnected nearby nodes. In real traffic network upgrade scenarios, the physical locations of candidate hubs are fixed. Normal communication modules have limits on maximum transmission power and Line-of-Sight (LoS for brief). To build a normal cooperative link between any two hubs $\mathcal{V}_i$ and $\mathcal{V}_j$, their Euclidean distance must meet a hard hardware constraint:

$$d_{ij} \leq D_{\max}. \tag{15}$$

Under the strict local spatial constraints of Equation (15), classic conclusions in graph theory and network science show a fact. The algebraic connectivity $\lambda_2$ of spatial networks (like random geometric graphs) will drop sharply by $O(1/N)$ as the network size $N$ grows [36]. Such topology connectivity clearly cannot meet the needs of UAV scheduling agents for high-frequency global negotiation. Therefore, under a limited budget, we must allow hardware upgrades like installing directional antennas. This breaks the $D_{\max}$ limit between a few key hubs to build cross-regional super-long backbone links.

Based on these real-world thoughts, the actual topology design turns into a combinatorial optimization problem. It has geometric conditions and hardware budgets. We are given an initial connected network limited by $D_{\max}$. Its graph Laplacian matrix is $L_0$. We also have $k$ allowed new directional antenna links. We define the global candidate edge set as $\mathcal{F} = \{e = (\mathcal{V}_i, \mathcal{V}_j) \mid (\mathcal{V}_i, \mathcal{V}_j) \notin \mathcal{E}_0\}$. The strategic planning problem can be written as the following nonlinear optimization:

$$\begin{aligned} \max_{E \subseteq \mathcal{F}} \quad & \lambda_2(L_0 + L_E) \\ \text{s.t.} \quad & |E| = k, \quad \text{(Construction budget constraint)} \\ & L_E = \sum_{e \in E} (\mathbf{e}_i - \mathbf{e}_j)(\mathbf{e}_i - \mathbf{e}_j)^\top. \end{aligned} \tag{16}$$

Here, $L_0 + L_E = L^*$ is the graph Laplacian matrix of the final topology $\mathcal{G}^*$ after adding the edge set $E$. Solving Equation (16) is an NP-Hard problem [37]. This paper proposes a greedy incremental edge-adding algorithm using the Fiedler vector to efficiently get a high-quality approximate solution.

For the Laplacian matrix $L$ of the current network, let $\mathbf{f}$ be the orthonormal eigenvector corresponding to $\lambda_2$. This vector is also called the Fiedler vector. It satisfies $\|\mathbf{f}\|_2 = 1$ and $\mathbf{f} \perp \mathbf{1}$. Suppose we try to add a feasible link $e = (\mathcal{V}_i, \mathcal{V}_j)$

## 5. Operational Layer: Multi-Agent Asynchronous Scheduling Algorithm Tolerating Incomplete Negotiation

The strategic layer planning in Section 4 shows a clear fact. Under a given physical degree limit, the Ramanujan topology network can provide algebraic connectivity $\lambda_2(L)$ approaching the theoretical limit. This section turns to the operational layer. Based on the UAV hub network built in Section 4, we design a high-demand distributed resource allocation algorithm for multi-agent systems.

To ensure multi-hub task allocation strictly meets $0-1$ integer constraints, the mathematical model built in Section 3 must keep a strict linear form. However, linear objective functions are not strictly convex. Besides, real traffic networks have inevitable asynchronous communication delays. These factors will cause severe numerical oscillations in traditional consensus algorithms. Therefore, this paper proposes a customized topology-aware asynchronous distributed ADMM (IC-AsyncADMM). It strictly breaks down the multi-agent cooperative problem into four core mathematical modules. They are local adaptive scheduling, decentralized network consensus, asynchronous interaction conservation, and anti-noise residual balance.

### *5.1. Local Scheduling: Distributed Augmented Lagrangian and Adaptive Projection (x-update)*

In the decentralized scheduling architecture, each UAV hub is modeled as an autonomous scheduling agent with independent computing power. To decouple the global task demand constraint $\sum_{i=1}^{N} \mathbf{x}_i = \mathbf{1}$, we introduce a consensus variable $\mathbf{z}_i \in \mathbb{R}^M$. This represents the network-level allocation intent. We construct the distributed augmented Lagrangian function $\mathcal{L}_\rho$ for the multi-agent system:

$$\mathcal{L}_\rho(\{\mathbf{x}_i\},\{\mathbf{z}_i\},\{\mathbf{y}_i\}) = \sum_{i=1}^{N}\left(\mathbf{c}_i^\top \mathbf{x}_i + \mathbf{y}_i^\top(\mathbf{x}_i-\mathbf{z}_i) + \frac{\rho_i}{2}\|\mathbf{x}_i-\mathbf{z}_i\|_2^2\right), \tag{17}$$

Here, $\mathbf{y}_i \in \mathbb{R}^M$ is the dual multiplier to enforce the consensus constraint. $\rho_i > 0$ is the localized penalty parameter.

In the $k+1$ iteration of the outer ADMM, UAV hub $\mathcal{V}_i$ first updates its local scheduling strategy $\mathbf{x}_i^{k+1}$. This operation is strictly limited by the physical capacity feasible set $\tilde{\mathcal{X}}_i = \{\mathbf{x}_i \in \mathbb{R}^M \mid \mathbf{x}_i \geq \mathbf{0}, \mathbf{1}^\top \mathbf{x}_i \leq C_i\}$. After completing the square for Equation (17) and ignoring constant terms, we define the unconstrained optimal trend vector $\mathbf{v}_i$:

$$\mathbf{v}_i = \mathbf{z}_i^k - \frac{1}{\rho_i^k}(\mathbf{c}_i + \mathbf{y}_i^k). \tag{18}$$

Now, the subproblem is equivalent to accurately projecting $\mathbf{v}_i$ onto the feasible set $\tilde{\mathcal{X}}_i$:

$$\mathbf{x}_i^{k+1} = \arg\min_{\mathbf{x}_i \in \tilde{\mathcal{X}}_i} \frac{1}{2}\|\mathbf{x}_i - \mathbf{v}_i\|_2^2. \tag{19}$$

Since the feasible set $\tilde{\mathcal{X}}_i$ meets the Slater condition, the KKT conditions are both necessary and sufficient. We build the corresponding Lagrangian function. We introduce a scalar multiplier $\mu \geq 0$ for the capacity constraint and a vector multiplier $\boldsymbol{\lambda} \geq \mathbf{0}$ for the non-negative constraint:

$$\mathcal{L}_{proj}(\mathbf{x}_i, \mu, \boldsymbol{\lambda}) = \frac{1}{2}\|\mathbf{x}_i - \mathbf{v}_i\|_2^2 + \mu(\mathbf{1}^\top \mathbf{x}_i - C_i) - \boldsymbol{\lambda}^\top \mathbf{x}_i. \tag{20}$$

Based on the stationary condition $\nabla_{\mathbf{x}_i}\mathcal{L}_{proj} = \mathbf{0}$ and the complementary slackness of the non-negative constraint $\lambda_j x_{ij} = 0$, we can eliminate $\lambda_j$ to get the truncation operator:

$$x_{ij} = \max(v_{ij} - \mu, 0). \tag{21}$$

Based on the complementary slackness of the capacity constraint $\mu(\mathbf{1}^\top \mathbf{x}_i - C_i) = 0$, the projection process has two cases: 1) Suppose the initial test vector $\tilde{\mathbf{x}}_i = \max(\mathbf{v}_i, \mathbf{0})$ meets $\mathbf{1}^\top \tilde{\mathbf{x}}_i \leq C_i$. This means the UAV hub currently has enough capacity. The shadow price $\mu = 0$. We directly output $\mathbf{x}_i^{k+1} = \tilde{\mathbf{x}}_i$. 2) Suppose the initial test shows an overload ($\mathbf{1}^\top \tilde{\mathbf{x}}_i > C_i$). There must be a strictly active constraint $\mu > 0$. Substituting Equation (21) into the capacity equation, we need to solve the following nonlinear equation for the unique root $\mu^*$:

$$\sum_{j=1}^{M} \max(v_{ij} - \mu^*, 0) = C_i. \tag{22}$$

In algorithm implementation, the agent sorts $\mathbf{v}_i$ in descending order. It uses a linear search to find the minimum cutoff index to determine $\mu^*$. The time complexity of this descending water-filling mechanism is $O(M \log M)$. It fits the computing power limits of early UAV hub processors.

### 5.2. Global Cooperation: Network Consensus Negotiation and Dual Update (z-update & y-update)

After updating local scheduling intents, the multi-agent system must negotiate globally. This ensures the unique allocation of macro tasks. We fix $\mathbf{x}^{k+1}$ and $\mathbf{y}^k$. The optimization subproblem for the consensus variable $\mathbf{z}$ is defined as:

$$\begin{aligned} \min_{\{\mathbf{z}_i\}} \quad & \sum_{i=1}^{N} \frac{\rho_i^k}{2} \left\| \mathbf{z}_i - \left( \mathbf{x}_i^{k+1} + \frac{1}{\rho_i^k} \mathbf{y}_i^k \right) \right\|_2^2 \\ \text{s.t.} \quad & \sum_{i=1}^{N} \mathbf{z}_i = \mathbf{1}. \end{aligned} \tag{23}$$

We define the comprehensive state vector $\mathbf{q}_i = \mathbf{x}_i^{k+1} + \frac{1}{\rho_i^k} \mathbf{y}_i^k$. We build the Lagrangian function and introduce the dual multiplier $\boldsymbol{\nu} \in \mathbb{R}^M$ for the global coupling constraint. Based on the first-order stationarity condition, we eliminate the multiplier $\boldsymbol{\nu}$ (assuming a uniform penalty parameter $\rho_i^k = \rho$ across the network). We get the analytical update formula:

$$\mathbf{z}_i^{k+1} = \mathbf{q}_i - \bar{\mathbf{q}} + \frac{1}{N} \mathbf{1}, \tag{24}$$

Here, $\bar{\mathbf{q}} = \frac{1}{N} \sum_{j=1}^{N} \mathbf{q}_j$ is the average value of comprehensive states across the whole network. Then, agents execute the standard dual ascent:

$$\mathbf{y}_i^{k+1} = \mathbf{y}_i^k + \rho_i^k (\mathbf{x}_i^{k+1} - \mathbf{z}_i^{k+1}). \tag{25}$$

Equation (24) requires isolated agents to get the global average. In a decentralized architecture, this requirement must rely on information interaction through the local physical communication topology $\mathcal{G}$ to approximate.

### 5.3. Asynchronous Interaction: Incomplete Communication Conservation Mechanism Based on Poisson Clock

To calculate the global average $\bar{\mathbf{q}}$ in the decentralized topology $\mathcal{G} = (\mathcal{V}, \mathcal{E})$, we need to start an inner loop of pure communication inside the outer iteration step. In the physical world, it is extremely hard to require a consistent global clock. Therefore, this paper uses an asynchronous interaction model. That means in a specific time frame, there is only one interaction between UAV hubs.

We introduce a Poisson clock with a running rate of $\lambda > 0$ for each physical link $e \in \mathcal{E}$. In the $t$-th bilateral negotiation event, if link $(\mathcal{V}_i, \mathcal{V}_j)$ is activated, the network cascaded state matrix $\mathbf{U}(t) = [\mathbf{w}_1(t), \ldots, \mathbf{w}_N(t)]^\top$ updates according to the single-step transition matrix: $\mathbf{U}(t+1) = \mathbf{W}(t)\mathbf{U}(t)$. Here,

$$\mathbf{W}(t) = I - \frac{1}{2} (\mathbf{e}_i - \mathbf{e}_j)(\mathbf{e}_i - \mathbf{e}_j)^\top. \tag{26}$$

Taking the expectation of the single-step transition matrix reveals its isomorphic relationship with the physical Laplacian matrix $L$:

$$\mathbb{E}[\mathbf{W}(t)] = I - \frac{1}{2|E|} L. \tag{27}$$

Since $L\mathbf{1} = \mathbf{0}$, the transition matrix $\mathbf{W}(t)$ is strictly doubly stochastic ($\mathbf{1}^\top \mathbf{W}(t) = \mathbf{1}^\top$). We define the instantaneous global average row vector $\bar{\mathbf{u}}(t)^\top = \frac{1}{N} \mathbf{1}^\top \mathbf{U}(t)$. Its conditional expectation satisfies:

$$\mathbb{E}[\bar{\mathbf{u}}(t+1)^\top \mid \mathbf{U}(t)] = \bar{\mathbf{u}}(t)^\top. \tag{28}$$

This shows that the multi-dimensional average sequence forms a strict martingale. From an engineering perspective, this property means the total mass of the multi-agent system states is absolutely conserved during asynchronous interaction. Actual communication may be cut off early due to delays and not fully converge. However, the consensus $\mathbf{z}$ calculated based on the estimated average with residual noise still strictly meets $\sum_{i=1}^{N} \mathbf{z}_i = \mathbf{1}$ in expectation. This fundamentally prevents task omissions.

To quantify the convergence rate, we define the consensus error matrix $\mathbf{E}(t) = \mathbf{U}(t) - \mathbf{1}\bar{\mathbf{q}}^\top$. Since the average has been removed, we can use the trace property $\|\mathbf{E}\|_F^2 = \mathrm{Tr}(\mathbf{E}^\top\mathbf{E})$ and the Rayleigh quotient condition. The expected energy evolution of the error system is:

$$\mathbb{E}[\|\mathbf{E}(t)\|_F^2] \leq \left(1 - \frac{\lambda_2(L)}{2|E|}\right)^t \|\mathbf{E}(0)\|_F^2. \tag{29}$$

Equation (29) shows the role of algebraic connectivity in the global negotiation of the multi-agent system. The estimated variance shows a strict exponential decay. Its base is completely dominated by the algebraic connectivity $\lambda_2(L)$ of the physical network topology.

### *5.4. Anti-Noise Mechanism: Topology-Aware Initialization and EMA Residual Adaptation*

Under asynchronous communication with incomplete negotiation, UAV hubs inevitably produce estimation errors when getting the average of the global consensus variable $\mathbf{z}$. This consensus state carries residual noise. When it passes to the outer ADMM iteration, it easily causes high-frequency oscillations of the purely linear objective function between the vertices of the local feasible region. To adaptively suppress this oscillation, we introduce a lemma based on the spectral condition number of quadratic optimization.

From Section 3, $\mathbf{c}_i \in \mathbb{R}^M$ is the local execution cost vector for hub $\mathcal{V}_i$. We define the original point-to-point cost matrix for the whole network as $\mathbf{C}^{raw} = [\mathbf{c}_1, \mathbf{c}_2, \ldots, \mathbf{c}_N]^\top$. To eliminate numerical instability caused by dimensional differences, we first do min-max normalization on $\mathbf{C}^{raw}$:

$$\mathbf{C} = \begin{cases} \dfrac{\mathbf{C}^{raw} - C_{\min}}{C_{\max} - C_{\min}}, & C_{\max} > C_{\min} + 10^{-5}, \\ \mathbf{0}, & \text{Otherwise}, \end{cases} \tag{30}$$

Here, $C_{\max} = \max_{i,j} C_{ij}^{raw}$ and $C_{\min} = \min_{i,j} C_{ij}^{raw}$. Based on this, we propose an adaptive penalty parameter initialization strategy. It considers both the cost scale and underlying topology features:

$$\rho_0 = \alpha \cdot \max\left(\frac{1}{N \cdot M}\sum_{i=1}^{N}\sum_{j=1}^{M}|C_{ij}|, 0.1\right) \cdot \sqrt{\lambda_2(L) \cdot \lambda_N(L)}, \tag{31}$$

Here, $\alpha$ is a scaling factor. $L$ is the communication network Laplacian matrix. $\lambda_2(L)$ and $\lambda_N(L)$ are its algebraic connectivity and maximum eigenvalue, respectively.

For a regular network with a maximum degree of $d$, its maximum Laplacian eigenvalue is strictly limited by the minimum eigenvalue of the adjacency matrix $\mu_{\min}(A)$. Specifically, in the network topology built in this paper, the upper bound of $\lambda_N(L)$ is firmly limited:

$$\lambda_N(L) = d - \mu_{\min}(A) \leq d + 2\sqrt{d-1} \leq 2d. \tag{32}$$

Equation (31) and Equation (32) together reveal a rule. The fluctuation of $\lambda_N(L)$ is very small. Therefore, the magnitude of the initial penalty parameter $\rho_0$ is essentially completely dominated by the algebraic connectivity $\lambda_2(L)$. This topology-aware initialization strategy is very important. At the start of the iteration, it injects the spectral properties of the physical infrastructure into the agent's algorithm core. It automatically balances the slowest consensus diffusion mode and the fastest local oscillation mode in the network. This establishes the optimal theoretical anchor for the subsequent dynamic residual balance.

After setting accurate initialization parameters, we need to deal with the network noise caused by incomplete negotiation. We further introduce Exponential Moving Average (EMA) technology to build an anti-noise residual filter:

$$\tilde{r}^{k+1} = \beta\|\mathbf{r}^{k+1}\|_2 + (1-\beta)\tilde{r}^k, \tag{33}$$

$$\tilde{s}^{k+1} = \beta\|\mathbf{s}^{k+1}\|_2 + (1-\beta)\tilde{s}^k, \tag{34}$$

Here, $\beta \in (0, 1)$ is the smoothing factor. The algorithm dynamically scales the penalty parameter $\rho$ based on the ratio of the filtered smoothed primal residual $\tilde{r}^{k+1}$ to the dual residual $\tilde{s}^{k+1}$. This EMA parameter iteration mechanism can

effectively filter out instant errors caused by single asynchronous communication cutoffs. It allows the system to keep the stability of the overall optimization direction even in poor communication environments where global average $\mathbf{z}$ is inaccurate.

However, we must point out a fact. If the underlying physical communication is cut off too severely, the global average calculation will be extremely inaccurate. This will inevitably prevent the algorithm from strictly converging to the optimal solution of the continuous relaxed model.

The complete distributed scheduling algorithm is shown in Algorithm 1.

**Algorithm 1** Multi-Agent Asynchronous Scheduling Algorithm Tolerating Incomplete Communication (IC-AsyncADMM)

**Require:** Physical interaction topology $\mathcal{G}$, cost vector set $\{\mathbf{c}_i\}$, hub capacity limit $\{C_i\}$, physical communication window $T_{\max}$

**Ensure:** Discrete multi-agent allocation strategy $\mathbf{x}^*$ meeting all constraints

**Initialize**: Strategy $\mathbf{x}_i, \mathbf{z}_i, \mathbf{y}_i \leftarrow \mathbf{0}$; Topology-aware penalty parameter $\rho_0 \leftarrow \sqrt{\lambda_2(L) \cdot \lambda_N(L)}$; Smoothed residuals $\tilde{r}, \tilde{s} \leftarrow 0$

**for** Outer ADMM iteration $k = 0, 1, 2, \ldots$ until convergence or cutoff **do**

  **/* Module 1: Local Scheduling and Adaptive Projection ($x$-update) */**

  **for** Each autonomous scheduling agent $\mathcal{V}_i \in \mathcal{V}$ **in parallel do**

    Calculate unconstrained scheduling trend: $\mathbf{v}_i \leftarrow \mathbf{z}_i^k - (\mathbf{c}_i + \mathbf{y}_i^k)/\rho_i^k$

    Find shadow price $\mu^*$ via water-filling method, execute local projection: $\mathbf{x}_i^{k+1} \leftarrow \max(\mathbf{v}_i - \mu^* \mathbf{1}, \mathbf{0})$

    Prepare negotiation state: $\mathbf{q}_i \leftarrow \mathbf{x}_i^{k+1} + \mathbf{y}_i^k/\rho_i^k$

  **end for**

  **/* Module 2: Incomplete Communication Inner Loop Based on Poisson Clock */**

  Trigger asynchronous bilateral negotiation across the network within the extremely short physical window $T_{\max}$:

    If link $(\mathcal{V}_i, \mathcal{V}_j)$ is activated, execute state averaging: $\mathbf{q}_i, \mathbf{q}_j \leftarrow \frac{1}{2}(\mathbf{q}_i + \mathbf{q}_j)$

  **/* Module 3: Network Consensus Negotiation and Dual Update ($z$ & $y$-update) */**

  **for** Each autonomous scheduling agent $\mathcal{V}_i \in \mathcal{V}$ **in parallel do**

    Get noisy average estimation after communication cutoff: $\tilde{\mathbf{q}}_i$

    State conservation algebraic compensation: $\mathbf{z}_i^{k+1} \leftarrow \mathbf{q}_i^{\text{init}} - \tilde{\mathbf{q}}_i + \frac{1}{N}\mathbf{1}$

    Local dual ascent: $\mathbf{y}_i^{k+1} \leftarrow \mathbf{y}_i^k + \rho_i^k(\mathbf{x}_i^{k+1} - \mathbf{z}_i^{k+1})$

  **end for**

  **/* Module 4: Anti-Noise EMA Residual Adaptation and Noise-Floor Cutoff */**

  Calculate global residuals, use Exponential Moving Average (EMA) to get anti-noise smoothed residuals $\tilde{r}^{k+1}$ and $\tilde{s}^{k+1}$

  Dynamically scale next round penalty parameter $\rho^{k+1}$ based on residual balance criteria

  **if** Smoothed primal residual $\tilde{r}^{k+1}$ falls into noise-floor stagnation **or** meets target accuracy **then**

    $\mathbf{x}^* \leftarrow \text{Heuristic}(\mathbf{x}^{k+1})$ ▷ Execute maximum trend discrete hard assignment to prevent stagnation

    **break**

  **end if**

**end for**

**return** $\mathbf{x}^*$

## 6. Experimental Validation: Strategic-Operational End-to-End Evaluation of Multi-Agent Logistics Networks

To verify the effectiveness of the proposed strategic-operational co-optimization framework, this section conducts four sets of experiments based on real delivery site geographical data. The experiment logic strictly follows the theoretical deduction path of this paper: (1) Infrastructure diagnosis: Empirical analysis of connectivity loss in existing delivery networks. (2) Strategic layer validation: Approximate Ramanujan topology reshaping based on real sites.

(3) Theoretical ablation: The leading role of algebraic connectivity in decentralized cooperative efficiency. (4) Operational layer validation: Scheduling efficiency evaluation in large-scale multi-agent systems tolerating incomplete communication.

### *6.1. Experiment 1 (Infrastructure Diagnosis): Empirical Analysis of Connectivity Loss in Existing Logistics Networks*

This experiment aims to evaluate the structural bottlenecks of directly reusing existing urban delivery sites as multi-agent cooperative scheduling infrastructure. We look at this from the perspective of physical network topology. The study extracted Point of Interest (POI for brief) data of secondary sites of six major delivery brands (SF Express, JD Logistics, ZTO, YTO, Yunda, J&T) in representative cities nationwide. After removing extreme and isolated samples, we set a communication and service coverage threshold of $R = 5$km for the remaining valid "city-brand" networks. If the geographical distance between two sites is less than this threshold, an undirected communication link is built in the topology graph.

To strictly quantify the network's potential to support decentralized cooperation, this experiment uses the algebraic connectivity $\lambda_2^{\text{real}}$ as the core metric. We also introduce the theoretical optimal bound of the Ramanujan graph $\lambda_2^{\text{opt}} = \bar{d} - 2\sqrt{\bar{d}-1}$ under the same node scale and average degree $\bar{d}$ as a baseline. Thus, we define the network connectivity loss rate as $\eta = \max\left(0, 1 - \lambda_2^{\text{real}}/\lambda_2^{\text{opt}}\right)$. This metric directly reflects the drop in global information interaction efficiency caused by uneven spatial layout in real networks.

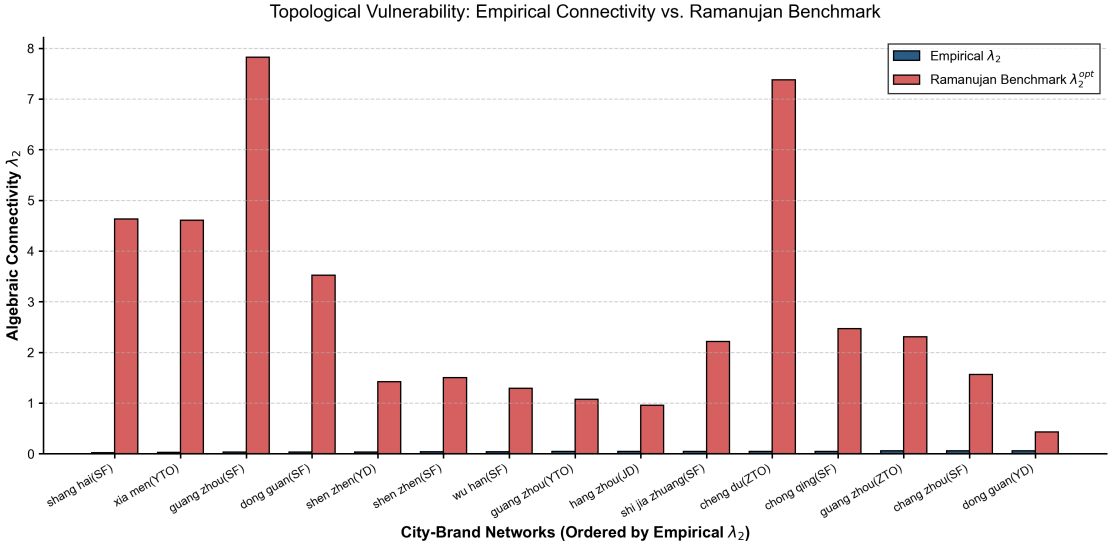



Figure 2: Gap analysis between real algebraic connectivity of city-brand networks and Ramanujan theoretical baselines

Figures 2 and 3 reveal the obvious defects of existing ground logistics infrastructure when converted into multi-agent communication networks. From the perspective of system connectivity, in almost all "city-brand" combinations, the algebraic connectivity of real networks is much lower than the theoretical optimal value under the same construction cost. The average connectivity loss rate of the overall network is up to 41.89%. The root cause of this high loss lies in the spatial clustering effect driven by business: logistics sites tend to form high-density cliques in core business districts. If we directly upgrade them into autonomous scheduling agents without modification, this highly heterogeneous spatial topology will easily cause information islands and long-tail delays during the multi-agent consensus convergence process. This provides a solid factual basis for implementing the subsequent strategic layer topology reshaping.

### *6.2. Experiment 2 (Strategic Layer Validation): Approximate Ramanujan Topology Reshaping under Spatial Constraints*

This experiment takes the real logistics network in Chengdu as an example. It aims to empirically verify the topology planning theory under spatial constraints proposed in Section 4. Specifically, it verifies the effectiveness of

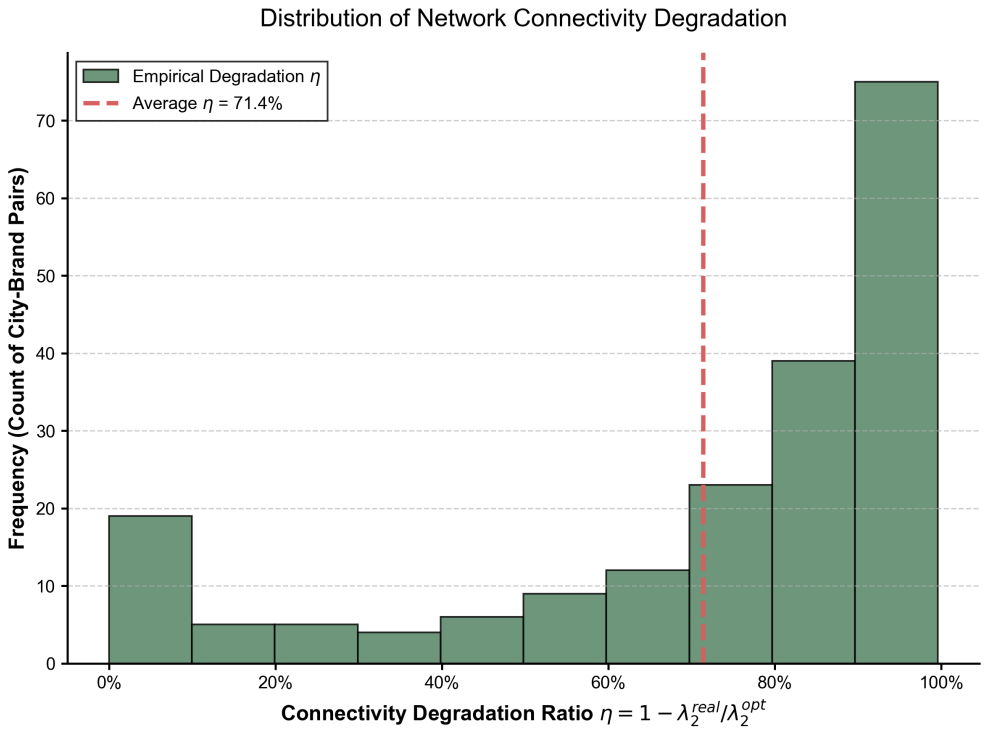



Figure 3: Distribution histogram of connectivity loss rate ($\eta$) in existing logistics networks ($R$ = 5km)

the Fiedler vector-based greedy incremental algorithm. It shows how the algorithm breaks the spatial clustering effect and approaches the Ramanujan connectivity limit under a limited infrastructure budget.

Through spatial uniform sampling and simulated annealing mapping, the study extracted $N = 100$ core secondary sites as candidate UAV communication hubs. Limited by the line-of-sight and transmission power of normal microwave communication hardware, the upper limit of the basic physical communication radius is set to $D_{\max} = 5$km. Figure 4 shows the initial topology driven purely by geographical distance (average degree $\bar{d} \approx 8$). It inevitably inherits a large number of local cliques and cross-regional communication breaks.

To break the connectivity bottleneck, the experiment introduces the Fiedler greedy planning algorithm. The infrastructure budget for new directional antennas (long-distance communication edges) is set to 10% of the total number of initial links. The optimized heterogeneous spatial deployment topology is shown in Figure 5. The added budget is not redundantly consumed in dense clusters. Instead, it accurately crosses geographical isolation zones and sews up the structural "chokepoints" of the network.

### *6.3. Experiment 3 (Ablation Study): The Leading Role of Algebraic Connectivity in Multi-Agent Global Negotiation*

This experiment aims to strictly verify the core conclusion from Section 5 at the micro-dynamic level. The conclusion is: "Under incomplete communication, the exponential decay base of the estimated variance in multi-agent systems is completely dominated by the algebraic connectivity of the physical network." To do this, we conducted Monte Carlo simulation analysis with strict control variables under real physical spatial constraints.

We used the real delivery network in Beijing as the anchor point. We kept the equivalent physical communication radius $R_c$ and node scale $N$ strictly unchanged. We reconstructed five sets of topology schemes with different spectral properties to simulate different physical infrastructure scenarios:

(0) **Original Real Topology** ($\lambda_2 = 0.07$): As the baseline network. It shows the current logistics infrastructure driven purely by geographical demands. It has many information islands.

(1) **Baseline Random Geometric Graph (RGG,** $\lambda_2 = 0.13$**)**: The standard baseline for spatial network research. It simulates purely random geographical deployment of UAV hubs under a given density.

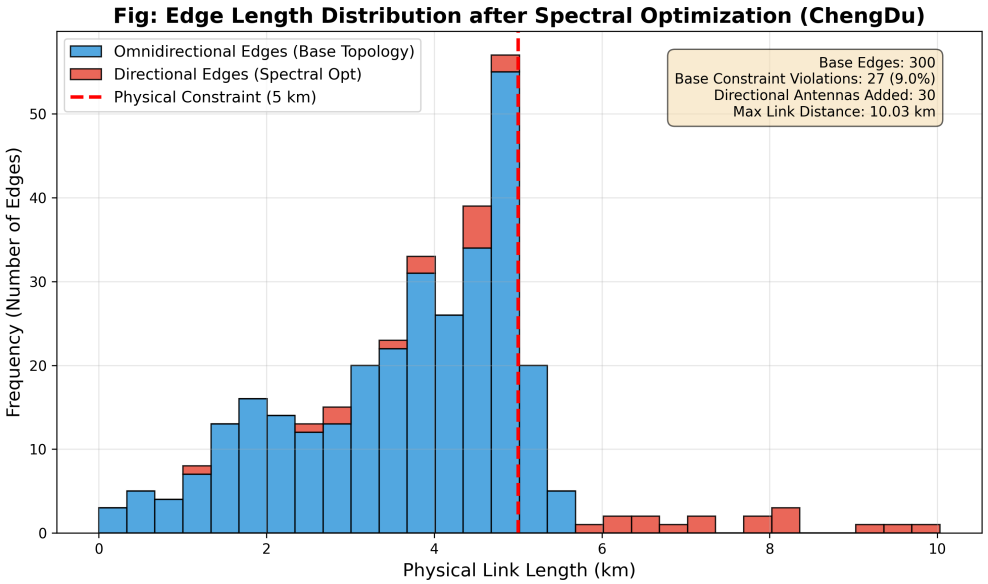



Figure 4: Link length distribution of the initial physical topology for UAV hubs in Chengdu (limited by $D_{\max}$ = 5km)

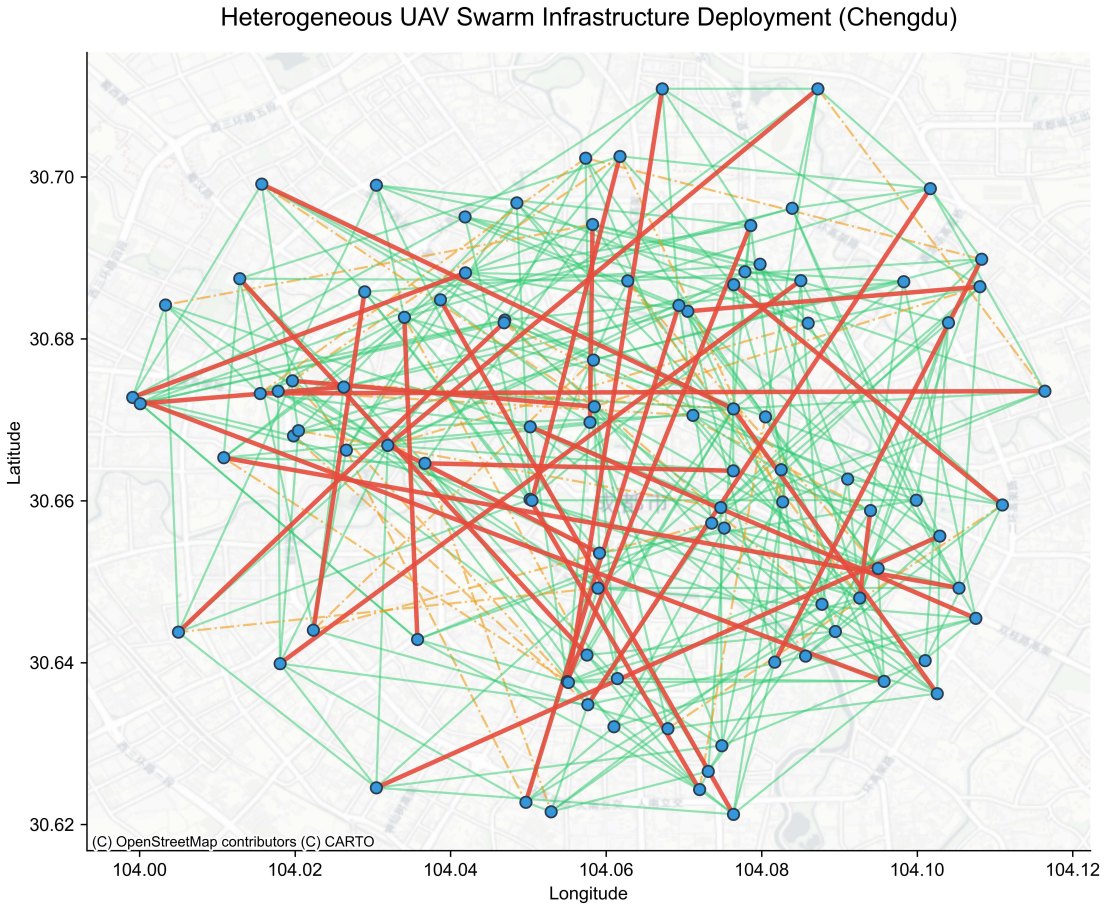



Figure 5: Heterogeneous deployment and long-edge injection topology of Chengdu UAV network hubs based on Fiedler spectral optimization

(2) **Strongly Clustered Topology** ($\lambda_2 = 0.02$): It simulates extreme commercial clustering effects (e.g., sites cluster strictly by business districts, with very few cross-district links). This causes severe topology bottlenecks.
(3) **Our Fiedler Optimized Topology** ($\lambda_2 = 0.76$): It follows the optimization logic in Section 6.2. Based on the original real topology, it uses our Fiedler greedy incremental algorithm to reshape a heterogeneous physical base by injecting a few directed long edges (10% budget).
(4) **Theoretical Ramanujan Limit** ($\lambda_2 = 2.01$): As the absolute physical limit. It represents a perfect expander graph built purely by algebraic graph theory, without any real geographical space limits.

Based on this, we deployed the multi-agent asynchronous decentralized negotiation protocol in the static topologies defined above. To eliminate random errors caused by Poisson clock activation, we ran 20 independent Monte Carlo simulations for each topology. This measures the complete dynamic process of a multi-agent system finishing one global negotiation (i.e., the network's mean squared error converges to the tolerance threshold).

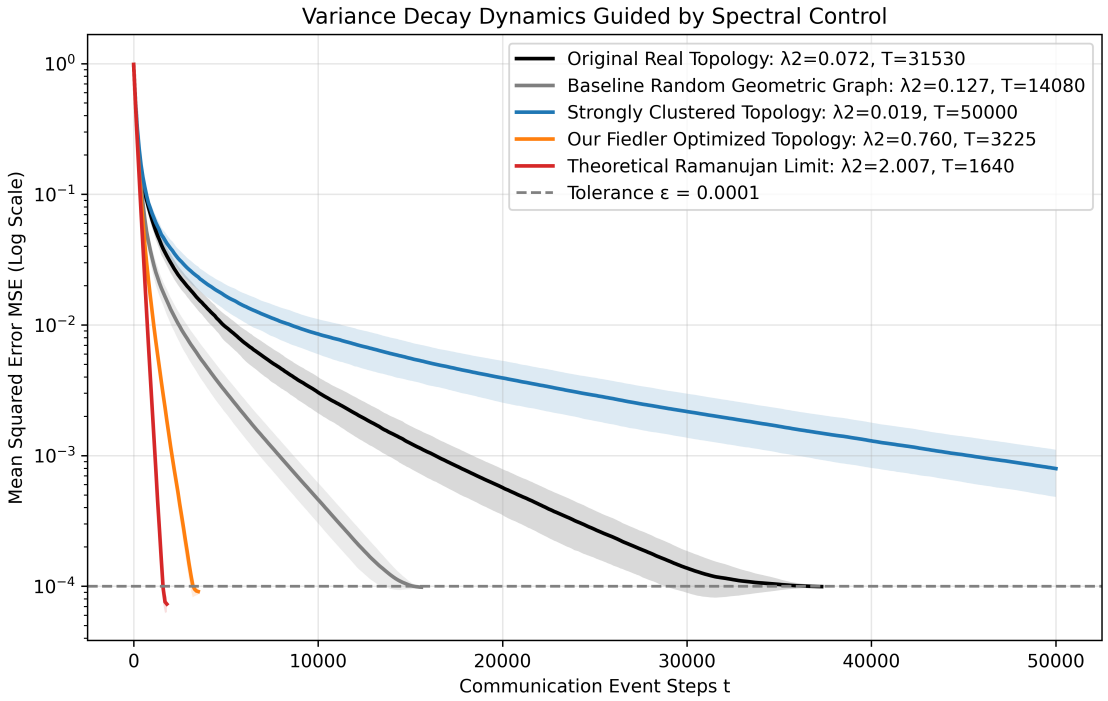



Figure 6: Decay dynamic trajectory of the Mean Squared Error (MSE) during asynchronous negotiation (Log scale, with confidence intervals)

Figure 6 shows the evolution trajectory of the system's Mean Squared Error (MSE for brief) over communication interaction steps. In the log-linear coordinate system, all curves show a clear linear drop. This perfectly proves the physical rule of exponential energy decay derived in theory. In the figure, the solid line represents the mean trajectory of 20 Monte Carlo simulations. The highlighted shaded area represents the standard deviation (confidence interval) caused by asynchronous communication randomness.

The slope of the convergence curve shows a very strict mathematical positive correlation with the algebraic connectivity $\lambda_2$ of each topology. Notably, our optimized topology (red solid line) and the Ramanujan limit not only drop very fast in mean value, but also have a very narrow shaded variance band. This proves that an underlying network with high $\lambda_2$ can not only accelerate negotiation, but also greatly absorb and smooth out random noise from incomplete asynchronous communication. It shows excellent engineering robustness.

Table 1 quantitatively compares the average mixing time needed for each scheme to make the network MSE reach the set tolerance threshold ($10^{-4}$). The extreme strongly clustered network has severe communication cuts. This easily causes local deadlocks for multi-agents. It takes over 50,000 steps and still cannot finish global negotiation. However, for our physical planning scheme reshaped by the Fiedler algorithm, the algebraic connectivity increases to 0.76. Its

Table 1: Comparison of multi-agent global negotiation time under different topology properties

| Topology Scheme | $\lambda_2(L)$ | Mean Negotiation Time (steps) | Speedup Ratio |
|---|---|---|---|
| 0. Original Real Network (Beijing) | 0.07 | 31530 | 1.0× (Baseline) |
| 1. Baseline RGG | 0.13 | 14080 | 2.2× |
| 2. Strongly Clustered Topology | 0.02 | >50000 | Slower than baseline |
| 3. **Our Fiedler Optimized Topology** | **0.76** | **3225** | **9.8**× |
| 4. Theoretical Ramanujan Limit | 2.01 | 1640 | 19.2× |

system cooperation time drops sharply from 31,530 steps in the original network to 3,225 steps. This achieves a system-level speedup of 9.8 times.

This ablation study proves that we must reshape the topology when upgrading delivery networks into multi-agent networks. It completely closes the logical loop from "underlying infrastructure topology planning" to "upper-layer multi-agent scheduling performance".

### *6.4. Experiment 4 (Operational Scheduling): Scheduling Experiments in Large-Scale Multi-Agent Networks*

This section conducts comprehensive experiments. It aims to verify the real engineering efficiency of our Incomplete-Communication Asynchronous ADMM (IC-AsyncADMM) algorithm when handling super-large-scale multi-agent cluster scheduling. This is based on the UAV hub network built by "spectral optimized layout" at the strategic layer.

*Experiment Setup and Baseline Comparison Mechanism.* The experiments cover multi-level hub scales from $N = 100$ to $N = 700$. To match real high-demand scenarios, test instances randomly generate sudden order demands that are 10 to 20 times the number of nodes. Furthermore, to remove randomness from a single experiment, we ran 20 independent Monte Carlo simulations for different scale hubs based on the same order demands.

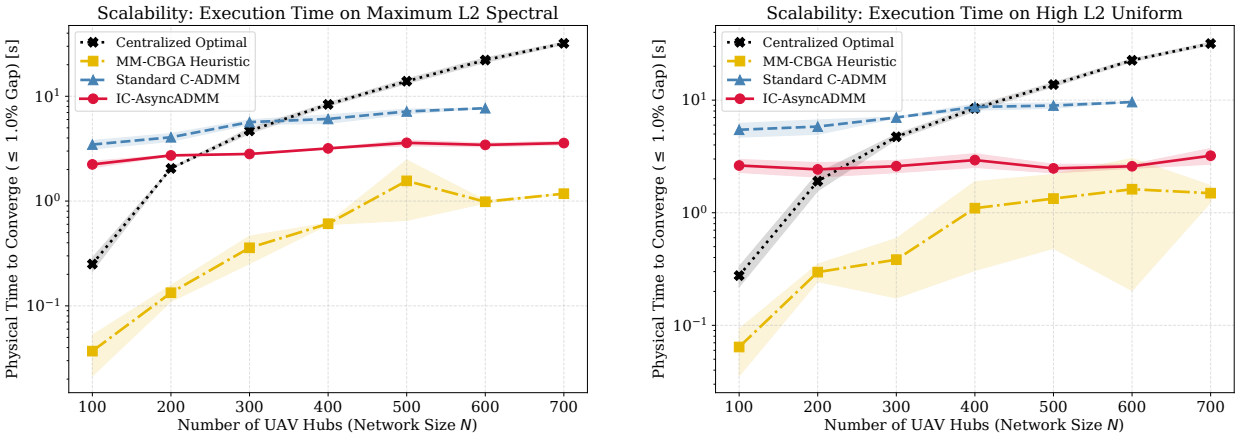
To fully evaluate the advancement of our framework, we introduce three strong baselines with fundamental differences in optimization mechanisms: 1) **Centralized Optimal (GT)**: We call the Gurobi solver to get the absolute exact solution from an omniscient view. The time complexity of the centralized architecture is $O(N^3)$, but it gets the exact optimal solution. Therefore, we choose it as a baseline to compare the accuracy and efficiency of different methods.

2) **Heuristic Multi-Agent Consensus-Based Bundle Algorithm (MM-CBGA)**: This is based on the latest CBBA variant proposed by Picard [38]. As a heuristic method based on greedy auction mechanisms, its biggest advantage is very fast interaction convergence speed. However, this algorithm lacks strict mathematical optimality guarantees. Under highly coupled capacity constraints, the accuracy of its solution often has randomness and is hard to stably approach the global optimum.

3) **Standard Consensus ADMM (Standard C-ADMM)**: This is based on the latest consensus ADMM framework improved for multi-UAV edge computing scenarios [39]. As a control group, this baseline mainly shows two mismatches of non-improved ADMM algorithms in real traffic scenarios. First, it lacks targeted upgrades for the underlying physical interaction topology. It cannot turn the fixed geographical locations of traffic infrastructure into an algorithm advantage. Second, its $z$-update step forces the calculation of an absolute exact global average. Under the incomplete negotiation environment in actual physical scenarios, mean errors easily cause huge synchronous waiting delays.

The core evaluation metric is Wall-clock Time, which strictly reflects physical passing time. This metric follows the physical mapping rule: $T = (T_{compute}/N) + T_{comm_delay}$. Here, the local microprocessor computing time is stripped through parallelization. The communication delay is pre-measured by the Gossip simulation engine determined by the underlying Poisson clock mechanism and bandwidth limits.

We must point out that the algorithm actually uses parallel computing in real scenarios. When readers reproduce the experiments, please simulate parallel computing and get the actual running time of the algorithm according to the parallel computing mode. In addition, the time of the centralized algorithm is the time to directly get the exact value. For MM-CBGA, it is the time to output its heuristic sub-optimal solution. For C-ADMM and our IC-AsyncADMM algorithm, the time is strictly defined as the time needed to reach the target accuracy of Gap $\leq 1\%$ compared to the optimal solution from the centralized algorithm.




(a) Theoretical Ramanujan Limit

(b) Our Fiedler Optimized Topology

Figure 7: System-level scalability evaluation: The evolution of physical passing time required to converge to 1% error with node scale $N$

Figure 7 shows the absolute physical time needed for each algorithm to reach the set accuracy target under two high-performance topologies.

As shown in the figure, the time complexity of the centralized algorithm is the highest among all algorithms. It is only fast in small-scale experiments. MM-CBGA shows lower time costs, but its computing time is only stable in theoretically optimal topologies. In our proposed topology matching physical scenarios, its running time oscillates significantly. And as mentioned before, its faster solving speed is at the cost of sacrificing accuracy. For Standard C-ADMM, which has a theoretical guarantee of exact convergence, it does not optimize parameters for the actual physical topology of agents. It also demands absolute accuracy of the global average. Its solving speed is obviously worse than our method.

In addition, it should be added that under $N = 600$, Standard C-ADMM only converged to a feasible solution with Gap=1% within the set iteration rounds 4 times. At $N = 700$, it failed to converge to a feasible solution within the set rounds in all 10 experiments.

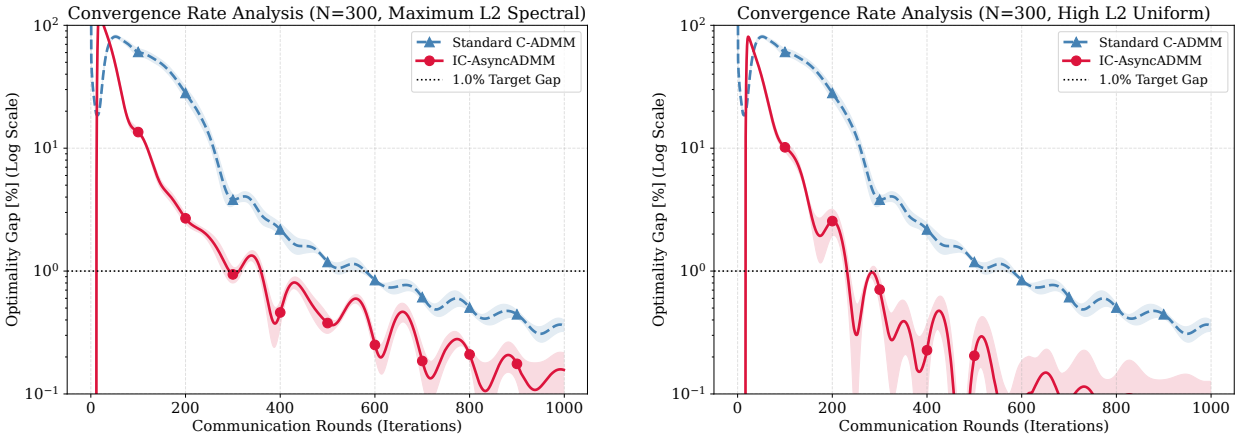
In contrast, our IC-AsyncADMM algorithm shows excellent scalability. On one hand, the spectral-aware initialization parameter $\rho_0$ cleverly injected through Equation (31) makes the algorithm keep an excellent low-order polynomial convergence slope under different scales. On the other hand, thanks to the EMA anti-noise mechanism, the algorithm can safely cut off useless communication and still keep high-accuracy iteration under incomplete negotiation.

In the super-large-scale network of $N = 700$, our method achieves a significant time reduction compared to Standard C-ADMM. Its response speed even approaches the heuristic MM-CBGA algorithm, which trades accuracy for speed. This shows that co-optimizing the topology network and scheduling algorithm on a good physical topology brings much better results in real traffic scenarios.

Figure 8 further shows the system residual evolution details under incomplete negotiation at the $N = 300$ scale. We can see that the residuals of our IC-AsyncADMM vary relatively largely in different Monte Carlo experiments. However, even under the sub-optimal Topology (Our Fiedler Optimized Topology), the algorithm still converges quickly.

This is because the EMA mechanism successfully cuts off useless computing loops and high-frequency communication bandwidth losses at the edge of convergence. It ensures the real-time, high-accuracy, and safe output of the scheduling plan in harsh environments.

What's more, to validate the practical feasibility of our proposed approach, we construct a small-scale urban scenario comprising $N = 100$ heterogeneous UAV hubs and $M = 200$ spatially distributed logistics demand points. As illustrated in Fig. 9, the spatial matching yields a highly efficient resource allocation topology. The directed links confirm that our strategy successfully serves all target demands while strictly adhering to the maximum service capacity constraints of the individual hubs, minimizing the global Euclidean distance overhead.




(a) Theoretical Ramanujan Limit

(b) Our Fiedler Optimized Topology

Figure 8: Convergence dynamic analysis: The drop trajectory of Optimality Gap with asynchronous communication interaction rounds

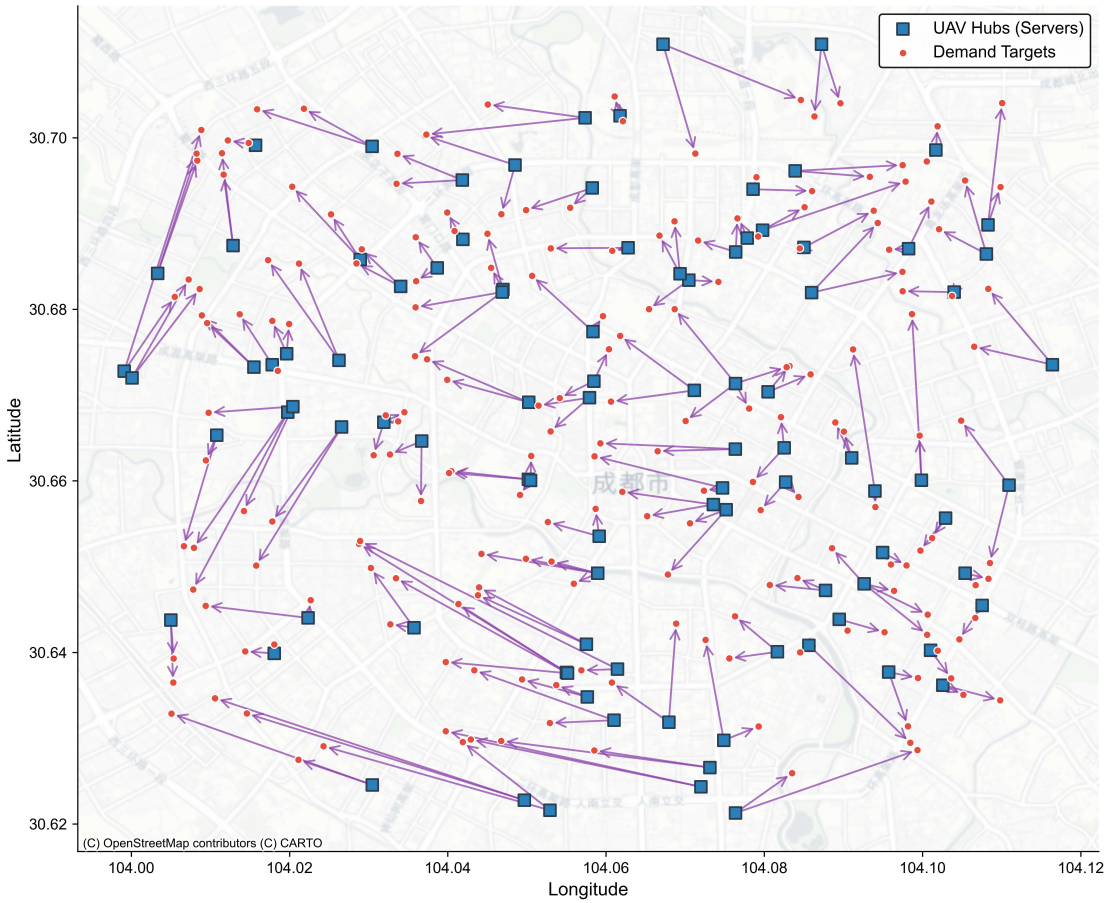



Figure 9: Visualization of the resource allocation strategy in a small-scale urban scenario. The blue squares represent the UAV hubs ($N = 100$), and the red circles indicate the logistics demand points ($M = 200$). The directed arrows demonstrate the optimized service links.

## 7. Conclusion and Future Work

This paper studies the topology planning of UAV logistics hubs based on upgrading existing delivery sites. The core insight is: the algebraic connectivity of the communication topology directly controls the convergence speed of distributed algorithms. Therefore, infrastructure planning should actively optimize spectral properties to accelerate distributed computing. Based on this insight, we propose a greedy incremental algorithm to build a Highly efficient UAV hub topology under geographical constraints. We also propose a topology-aware adaptive asynchronous ADMM algorithm.

Four sets of experiments based on real delivery site data fully verify the effectiveness of our methods. The conclusions are: existing delivery networks do have severe connectivity losses. Our method can reshape the logistics network under geographical constraints and significantly improve the algebraic connectivity. This makes the network fit the requirements of multi-agent distributed scheduling. It also increases the convergence speed of distributed scheduling by nearly an order of magnitude.

Future research directions include: (1) Extending the framework to dynamic scenarios with online hub adjustments; (2) Considering the joint decision-making of topology planning and fleet size optimization; (3) Testing our method on a real physical UAV logistics test platform to verify the performance improvement in actual operation.

## Appendix

**Lemma 2** (Integral Optimality of the Relaxed Assignment LP)**.** *Suppose the capacity parameter of each hub is $C_i \in \mathbb{Z}_{\geq 0}$. The constraint matrix of the model forms a bipartite graph incidence matrix and satisfies total unimodularity. Therefore, all extreme point solutions of the above continuous linear programming are naturally integer vectors. Thus, continuous relaxation does not change the optimal solution of the original integer programming problem. That is, $\mathbf{x}_i^* \in \{0,1\}^M$ automatically holds.*

*Proof.* We write the global demand constraint (6) and capacity constraint (7) in a compact matrix form:

$$\mathbf{A}\mathbf{x} \sim \mathbf{b}.$$

Here, $\mathbf{x} = [\mathbf{x}_1^\top, \ldots, \mathbf{x}_N^\top]^\top \in \mathbb{R}^{NM}$.

The matrix $\mathbf{A} \in \{0,1\}^{(N+M)\times NM}$ can be seen as the incidence matrix of a bipartite graph. This graph connects the hub node set $\mathcal{V}$ and the task node set $\mathcal{D}$. Each column represents a "task-hub" allocation variable. It has exactly one non-zero element in the task demand row and one non-zero element in the hub capacity row.

Note that matrix $\mathbf{A}$ meets the Heller-Tompkins conditions:

- Each column has exactly two non-zero elements.
- The rows can be divided into two disjoint subsets: task demand rows and hub capacity rows.
- The two non-zero elements in each column fall into different subsets.

Therefore, matrix $\mathbf{A}$ is a Totally Unimodular (TU) matrix.

Furthermore, we introduce slack variables to change the capacity inequality (7) into an equality form. We get the extended matrix:

$$[\mathbf{A}, \mathbf{I}] = \begin{bmatrix} \mathbf{A}_M & 0 \\ \mathbf{A}_N & \mathbf{I}_N \end{bmatrix}. \tag{.1}$$

Here, $\mathbf{A}_M$ and $\mathbf{A}_N$ represent the global demand constraint and capacity constraint, respectively. $\mathbf{I}_N$ is an identity matrix of size $N$. Adding an identity matrix to a TU matrix keeps the total unimodularity. Thus, $[\mathbf{A}, \mathbf{I}]$ is still a TU matrix.

Also, the right-hand vector is:

$$\mathbf{b} = [\mathbf{1}^\top, C_1, \ldots, C_N]^\top. \tag{.2}$$

This is a non-negative integer vector. According to the Hoffman-Kruskal theorem, all extreme points of the feasible polyhedron defined by $\mathcal{P} = \{\mathbf{x} \mid \mathbf{A}\mathbf{x} \sim \mathbf{b}, \mathbf{x} \geq 0\}$ are integer points.

The objective function (5) is a linear function. The optimal solution of the linear programming must lie at an extreme point of the feasible polyhedron $\mathcal{P}$. Therefore, this optimal solution must be an integer solution. Combined with the constraint structure, $\mathbf{x}_i$ must be a 0-1 vector. Thus, the continuous relaxation is exact. □

**Theorem 1** (Theoretical Upper Bound of Algebraic Connectivity for UAV Hubs)**.** *Given a physical construction constraint $d \geq 3$, suppose we have a connected $d$-bounded network topology $\mathcal{G}_N$ with $N$ UAV hubs. Its algebraic connectivity $\lambda_2(L)$ strictly meets the following bound:*

$$\lambda_2(L) \leq d - 2\sqrt{d-1} + O\left(\frac{1}{\log_{d-1} N}\right). \tag{13}$$

*Specifically, when the number of nodes $N \to \infty$ in the urban UAV logistics network, the system's algebraic connectivity has an asymptotic supremum (Alon-Boppana Bound):*

$$\limsup_{N\to\infty} \lambda_2(L) \leq d - 2\sqrt{d-1}. \tag{14}$$

*Proof.* First, we expand the communication links in the original physical topology. Let $\mathcal{G}_N = (\mathcal{V}, \mathcal{E})$ be any connected $d$-bounded graph with $N$ nodes. Its graph Laplacian matrix is $L_{\mathcal{G}}$. Suppose hardware constraints allow it. We add a communication link $e = (i, j) \notin \mathcal{E}$ between any two non-adjacent hubs $i$ and $j$ in the topology. We then get a new enhanced network topology $\mathcal{G}_N^+ = (\mathcal{V}, \mathcal{E} \cup \{e\})$.

The relationship between the Laplacian matrix $L_{\mathcal{G}^+}$ of the new topology and $L_{\mathcal{G}}$ of the original topology is shown in Equation (.3):

$$L_{\mathcal{G}^+} = L_{\mathcal{G}} + L_e = L_{\mathcal{G}} + (\mathbf{e}_i - \mathbf{e}_j)(\mathbf{e}_i - \mathbf{e}_j)^\top. \tag{.3}$$

Here, $I_N = (\mathbf{e}_1, \mathbf{e}_2, \ldots, \mathbf{e}_N)$. $\mathbf{e}_i \in \mathbb{R}^N$ is the $i$-th standard basis vector. For any state vector $\mathbf{x} \in \mathbb{R}^N$, its quadratic form $\mathbf{x}^\top L_e \mathbf{x} = (x_i - x_j)^2 \geq 0$ always holds. Thus, the incremental matrix $L_e$ is strictly positive semi-definite (i.e., $L_e \succeq 0$).

According to Equation (3), the algebraic connectivity of the new network topology $\mathcal{G}_N^+$ is shown in Equation (.4):

$$\lambda_2(L_{\mathcal{G}^+}) = \min_{\mathbf{x}\perp\mathbf{1}, \|\mathbf{x}\|_2=1} \mathbf{x}^\top L_{\mathcal{G}^+} \mathbf{x}. \tag{.4}$$

Let $\mathbf{x}^*$ be the optimal unit eigenvector that minimizes Equation (.4). We substitute the matrix addition and expand it to get:

$$\begin{aligned}
\lambda_2(L_{\mathcal{G}^+}) &= (\mathbf{x}^*)^\top (L_{\mathcal{G}} + L_e)\mathbf{x}^* \\
&= (\mathbf{x}^*)^\top L_{\mathcal{G}} \mathbf{x}^* + (\mathbf{x}^*)^\top L_e \mathbf{x}^* \\
&\geq (\mathbf{x}^*)^\top L_{\mathcal{G}} \mathbf{x}^* && (.5) \\
&\geq \min_{\mathbf{x}\perp\mathbf{1}, \|\mathbf{x}\|_2=1} \mathbf{x}^\top L_{\mathcal{G}} \mathbf{x} && (.6) \\
&= \lambda_2(L_{\mathcal{G}}).
\end{aligned}$$

Equations (.5) to (.6) show a clear fact. In the physical topology of UAV hubs, adding any effective communication link will not decrease the system's algebraic connectivity $\lambda_2(L)$. Therefore, for the original physical topology $\mathcal{G}$, we can continuously add communication links until $\deg(\mathcal{V}_i) = d$ for all $\mathcal{V}_i \in \mathcal{V}$. At this time, the physical topology $\mathcal{G}$ is called a $d$-regular graph.

For the finite $N$-node $d$-regular graph $\mathcal{G}$ after adding links, Nilli constructed a specific test vector attached to the network diameter $D$. He strictly proved that the second largest eigenvalue $\mu_2(A)$ of the corresponding adjacency matrix $A$ has a finite lower bound. This is shown in Equation (.7). The elements in the adjacency matrix $A$ satisfy: if edge $(\mathcal{V}_i, \mathcal{V}_j) \in \mathcal{E}$, then $A_{ij} = 1$; otherwise, $A_{ij} = 0$.

$$\mu_2(A) \geq 2\sqrt{d-1} - \frac{2\sqrt{d-1} - 1}{\lfloor D/2 \rfloor}. \tag{.7}$$

For any $N$-node $d$-regular graph, its network physical diameter $D$ is limited by the Moore Bound in algebraic graph theory. It must satisfy $D \geq \log_{d-1}(N)$. Substituting this diameter lower bound into Equation (.7), we get the lower bound of the finite-scale adjacency spectrum: $\mu_2(A) \geq 2\sqrt{d-1} - O(1/\log_{d-1} N)$.

We introduce the spectral mapping theorem. Since graph $\mathcal{G}$ is a $d$-regular graph, the degree matrix is $D = dI$. The eigenvalues of the Laplacian matrix $L = dI - A$ correspond one-to-one with the eigenvalues of the adjacency matrix $A$. They satisfy the following relationship: $\lambda_i(L) = d - \mu_i(A)$. Substituting this mapping, we prove Equation (13). Taking the limit $N \to \infty$, the trailing infinitesimal goes to 0. We then get the asymptotic upper bound in Equation (14). □

**Theorem 2** (Optimal Infrastructure: Ramanujan Topology)**.** *Suppose all non-trivial adjacency eigenvalues of a d-regular traffic topology $\mathcal{G}$ satisfy $|\mu_i(A)| \leq 2\sqrt{d-1}$ $(i \geq 2)$. Then it is called a Ramanujan graph. Combined with the spectral mapping theorem, its algebraic connectivity exactly reaches the physical limit under the degree constraint: $\lambda_2(L) \geq d - 2\sqrt{d-1}$.*

*Proof.* This proof provides the deterministic construction steps for the Ramanujan graph:

First, to build the Ramanujan graph, we introduce the Special Linear Group over a finite field $\mathbb{Z}_q$ as the theoretical basis. We define the Special Linear Group $\mathrm{SL}(2,\mathbb{Z}_q)$ and the Projective Special Linear Group $\mathrm{PSL}(2,\mathbb{Z}_q)$ as shown in Equation (.8) and Equation (.9).

$$\mathrm{SL}(2,\mathbb{Z}_q) = \left\{ \begin{pmatrix} a & b \\ c & d \end{pmatrix} \middle| \, a,b,c,d \in \mathbb{Z}_q,\ ad - bc \equiv 1 \pmod{q} \right\}. \tag{.8}$$

$$\mathrm{PSL}(2,\mathbb{Z}_q) = \mathrm{SL}(2,\mathbb{Z}_q)/\{I,-I\}. \tag{.9}$$

Here, $\mathbb{Z}_q = \{1,2,\ldots,q-1\}$. Equation (.9) is defined as a quotient group. Intuitively, in $\mathrm{PSL}(2,\mathbb{Z}_q)$, if $A \in \mathrm{SL}(2,\mathbb{Z}_q)$, then matrix $A$ and $-A$ are treated as the same element. That is, a group element can be represented as $\{A,-A\}$.

Let the target group be $G \in \{\mathrm{SL}(2,\mathbb{Z}_q), \mathrm{PSL}(2,\mathbb{Z}_q)\}$. Its theoretical network scale $N(q)$ corresponds to the following:

$$N(q) = |G| = \begin{cases} q(q^2-1), & G = \mathrm{SL}(2,\mathbb{Z}_q) \\ \frac{1}{2}q(q^2-1), & G = \mathrm{PSL}(2,\mathbb{Z}_q). \end{cases} \tag{.10}$$

Second, according to the actual demand scale $N_{\text{target}}$ of the urban UAV network, we choose an appropriate scaling prime $q$ and target group $G$. This ensures the generated theoretical network scale meets $N(q) \geq N_{\text{target}}$. In UAV hub planning, we must keep the closure of algebraic group operations and the completeness of the graph spectrum. Therefore, the extra $N(q) - N_{\text{target}}$ nodes must be kept. They can be configured as virtual routing hubs with zero physical cost. Here, for convenience, we assume $G$ is the Projective Special Linear Group $\mathrm{PSL}(2,\mathbb{Z}_q)$.

Third, we establish a one-to-one mapping $T$ between the UAV hub group $\mathcal{V}$ and the Projective Special Linear Group $G$. We have $T(\mathcal{V}_i) = G_i$. Through this isomorphic mapping, the originally isolated hub entities get the algebraic structure of the finite field linear group. This lays the spatial foundation for subsequent routing edge connections based on group multiplication rules.

Next, based on Jacobi's four-square theorem, we solve the Diophantine equation $a_0^2 + a_1^2 + a_2^2 + a_3^2 = p$. Existing research proves that this equation has $p + 1 = d$ sets of specific integer solutions. Through the LPS construction method, a set of solutions is mapped into a $2 \times 2$ complex integer matrix. This is shown in Equation (.11).

$$A(a_0,a_1,a_2,a_3) = \begin{pmatrix} a_0 + ia_1 & a_2 + ia_3 \\ -a_2 + ia_3 & a_0 - ia_1, \end{pmatrix} \tag{.11}$$

We can construct these $d$ sets of solutions into a set of $2 \times 2$ complex integer matrices using the LPS method. Then, through a homomorphic mapping [], we map them into group $G$ to get the generator set $\mathcal{S}$.

Finally, for any two UAV hubs $\mathcal{V}_i, \mathcal{V}_j \in \mathcal{V}$ in the network, we build an edge $(\mathcal{V}_i, \mathcal{V}_j)$ between them if and only if they satisfy $T(\mathcal{V}_i)^{-1}T(\mathcal{V}_j) \in \mathcal{S}$.

For the graph $\mathcal{G} = (\mathcal{V}, \mathcal{S})$ generated by the above algebraic rules, its algebraic connectivity is analytically proven to perfectly reach the theoretical upper limit of $d - 2\sqrt{d-1}$. □

## Declarations

**Ethical Approval.** Not applicable.

**Funding.** This work is supported by the National Key R&D Program of China (2024YFE0214600) and the National Natural Science Foundation of China (52308449).

**Declaration of generative AI and AI-assisted technologies in the manuscript preparation process.** As the authors are not native English speakers, AI-assisted tools were used to improve the clarity and readability of the manuscript, including language editing and translation. All ideas, methods, and conclusions in this work are the responsibility of the authors.

## References


[1] M. A. Zamal, A. H. Schrotenboer, T. Van Woensel, End-to-end logistics in metropolitan areas: A stochastic dynamic order-assignment and dispatching problem, Transportation Research Part B: Methodological 199 (2025) 103249.

[2] L. Stuive, F. Gzara, Airspace network design for urban uav traffic management with congestion, Transportation Research Part C: Emerging Technologies 169 (2024) 104882.

[3] M. von der Burg, J. Kamphof, J. Soomers, A. Sharpanskykh, Towards next-generation airport surface movement operations using hierarchical-distributed multi-agent planning, Transportation Research Part C: Emerging Technologies 186 (2026) 105583.

[4] R. Olfati-Saber, Flocking for multi-agent dynamic systems: Algorithms and theory, IEEE Transactions on automatic control 51 (3) (2006) 401–420.

[5] K. Charters-Gabanek, N. Raimbault, P. V. Hall, Logistics and urban planning: a review of literature, Journal of Planning Education and Research 45 (3) (2025) 663–673.

[6] R. Olfati-Saber, R. M. Murray, Consensus problems in networks of agents with switching topology and time-delays, IEEE Transactions on automatic control 49 (9) (2004) 1520–1533.

[7] R. Chen, J. Li, Y. Huang, Z. Xiong, X. Wang, L. Shen, Communication-efficient asynchronous consensus with global harmonization for large-scale uav swarms, IEEE Transactions on Aerospace and Electronic Systems 62 (2025) 1394–1408.

[8] L. Zhou, S. Leng, T. Q. Quek, Verdt: A versatile digital twins framework for uavs-based industrial cyber-physical systems, IEEE Transactions on Mobile Computing.

[9] L. Wang, X. Deng, J. Gui, P. Jiang, F. Zeng, S. Wan, A review of urban air mobility-enabled intelligent transportation systems: Mechanisms, applications and challenges, Journal of Systems Architecture 141 (2023) 102902.

[10] Y. Lu, W. Zeng, W. Wei, W. Wu, H. Jiang, Urban air mobility vertiports: A bibliometric analysis of applications, challenges, and emerging directions, Applied Sciences 15 (20) (2025) 10961.

[11] J. Zhang, S. Cui, P. Zhu, L. Wang, Z. Sun, Q. Shao, Research on location-routing problem for logistics uavs based on bi-layer programming, N/A.

[12] C. C. Ditta, M. N. Postorino, Three-dimensional urban air networks for future urban air transport systems, Sustainability 15 (18) (2023) 13551.

[13] E. B. Onat, Urban air mobility: Infrastructure and operations, Ph.D. thesis, University of California, Berkeley (2024).

[14] A. Kiran, J. V. N. Ramesh, A. Quraishi, J. C. Patni, I. Keshta, H. Byeon, M. Raparthi, M. Sandhu, M. Soni, Tiny machine learning approach for grid-based monitoring of uav tracking and cyber-physical systems in hydraulic surveying, IEEE Transactions on Intelligent Transportation Systems 26 (9) (2024) 14029–14038.

[15] L. Zhong, Y. Liu, X. Deng, C. Wu, S. Liu, L. T. Yang, Distributed optimization of multi-role uav functionality switching and trajectory for security task offloading in uav-assisted mec, IEEE Transactions on Vehicular Technology 73 (12) (2024) 19432–19447.

[16] X. Zheng, D. Lin, P. Tang, S. He, Distributed spatial-temporal trajectory optimization for unmanned-aerial-vehicle swarm, Journal of Guidance, Control, and Dynamics 49 (3) (2026) 819–835.

[17] B. Qiu, W. Cheng, H. He, W. Zhang, Joint topology and power optimization for multi-uav collaborative secure communication, IEEE Transactions on Wireless Communications.

[18] N. S. Aybat, E. Y. Hamedani, A distributed admm-like method for resource sharing over time-varying networks, SIAM Journal on Optimization 29 (4) (2019) 3036–3068.

[19] M. Doostmohammadian, H. R. Rabiee, Momentum-based accelerated algorithm for distributed optimization under sector-bound nonlinearity, Journal of the Franklin Institute (2025) 107857.

[20] S. Shrestha, Communication-efficient distributed asynchronous admm, arXiv preprint arXiv:2508.12233.

[21] H. Doerks, P. Häusner, D. H. Escobar, J. Sjölund, Learning to accelerate distributed admm using graph neural networks, arXiv preprint arXiv:2509.05288.

[22] S. Young, S. Aksoy, J. Firoz, R. Gioiosa, T. Hagge, M. Kempton, J. Escobedo, M. Raugas, Spectralfly: Ramanujan graphs as flexible and efficient interconnection networks, in: 2022 IEEE International Parallel and Distributed Processing Symposium (IPDPS), IEEE, 2022, pp. 1040–1050.

[23] X. Li, X. Tao, G. Mao, Unbalanced expander based compressive data gathering in clustered wireless sensor networks, IEEE Access 5 (2017) 7553–7566.

[24] S. A. Camtepe, B. Yener, M. Yung, Expander graph based key distribution mechanisms in wireless sensor networks, in: 2006 IEEE international conference on communications, Vol. 5, IEEE, 2006, pp. 2262–2267.

[25] H. Deng, T. Wu, Research on the consensus convergence rate of multi-agent systems based on hermitian kirchhoff index measurement, Entropy 27 (10) (2025) 1035.

[26] P. Di Lorenzo, S. Barbarossa, Distributed estimation and control of algebraic connectivity over random graphs, IEEE Transactions on Signal Processing 62 (21) (2014) 5615–5628.

[27] D. Groß, O. Stursberg, Optimized distributed control and network topology design for interconnected systems, in: 2011 50th IEEE Conference on Decision and Control and European Control Conference, IEEE, 2011, pp. 8112–8117.

[28] S. Zhang, A. Pananjady, J. Romberg, A dual accelerated method for online stochastic distributed averaging: From consensus to decentralized policy evaluation, IEEE Transactions on Automatic Control.

[29] S. Lu, J. Liu, Fast consensus topology design via minimizing laplacian energy, in: 2024 IEEE 63rd Conference on Decision and Control (CDC), IEEE, 2024, pp. 6187–6192.

[30] F. Yang, N. Matni, Communication topology co-design in graph recurrent neural network based distributed control, in: 2021 60th IEEE Conference on Decision and Control (CDC), IEEE, 2021, pp. 3619–3626.

[31] P. Li, C. Chen, S. Zhu, X. Guan, Distributed optimization for estimation and communication co-design under bandwidth constraints, IEEE Transactions on Signal and Information Processing over Networks.

[32] Y. Wang, Q. Yang, F. Xiao, H. Fang, J. Chen, Accelerated optimized topology design in affine formation control using admm, IEEE Transactions on Network Science and Engineering.
[33] Y. Shen, Z. Zhu, Y. Huang, C. Yan, C. Zhuo, J. Xu, Bandwidth-aware network topology optimization for decentralized learning, arXiv preprint arXiv:2512.07536.
[34] M. Hasanzadeh, A. Kargarian, Dynamic quantum optimal communication topology design for consensus control in linear multi-agent systems, arXiv preprint arXiv:2602.06215.
[35] M. Fiedler, Algebraic connectivity of graphs, Czechoslovak mathematical journal 23 (2) (1973) 298–305.
[36] D. A. Spielman, S.-H. Teng, Spectral partitioning works: Planar graphs and finite element meshes, Linear Algebra and its Applications 421 (2-3) (2007) 284–305.
[37] D. Mosk-Aoyama, Maximum algebraic connectivity augmentation is np-hard, Operations Research Letters 36 (6) (2008) 677–679.
[38] G. Picard, Multi-agent consensus-based bundle allocation for multi-mode composite tasks, in: International Conference on Autonomous Agents and Multiagent Systems, 2023.
[39] R. Huang, W. Wen, Z. Zhou, C. Dong, C. Qiao, Z. Tian, X. Chen, Dynamic task offloading for multi-uavs in vehicular edge computing with delay guarantees: A consensus admm-based optimization, IEEE Transactions on Mobile Computing 23 (12) (2024) 13696–13712.